POLARISED FLUORESCENCE SPECTRAL AND ANISOTROPY STUDIES IN HUMAN BREAST TISSUES

A THESIS SUBMITTED

IN PARTIAL FULFILMENT OF THE REQUIREMENTS

FOR THE DEGREE OF

MASTER OF TECHNOLOGY

by

B. V. Laxmi

to the

LASER TECHNOLOGY PROGRAMME

INDIAN INSTITUTE OF TECHNOLOGY

KANPUR–208016 INDIA

MAY 2000

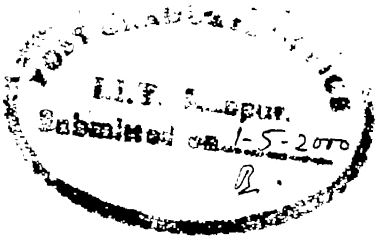

CERTIFICATE

It is certified that the work contained in the thesis entitled "***Polarised Fluorescence Spectral and Anisotropy Studies in Human Breast Tissues.***", by ***Miss. B. V. Laxmi*** , has been carried out under my supervision and that this work has not been submitted elsewhere for a degree.

A. Pradhan
Asst. Professor
Laser Technology Programme
I.I.T. Kanpur 208016

May, 2000

Dedicated to my beloved Mother

Contents:

Abstract:

In this project attempts are made to differentiate between normal, benign and malignant tumors of human breast tissues by extracting characteristic information from fluorescence shape profiles and depolarization effects. The major emphasize is flavin co-enzymes within the tissue, which are fluorescence active with Ar-ion laser excitation. Fluorescence properties of flavins have been investigated between 500nm to 700nm. Fluorescence anisotropy was estimated using the relation $r(\lambda)=(I_{\parallel}-I_{\perp})/(I_{\parallel}+2I_{\perp})$, where λ=530nm (flavin peak) . Samples are in the form of thick and thin slices of thickness 4mm to 0.5mm respectively. Analysis on the bandwidth of profiles revealed a distinct difference between normal, benign and malignant tumors. the specificity and sensitivity of 35 samples analysed are 95% and 94%. Lower anisotropy values of normal human breast tissues compared to benign or malignant tumors counterparts have been observed. Depolarization of any propagating light in turbid medium can occur due to multiple scattering. To reduce the effect of scattering in thick tissues experiments on thin tissues (0.5mm) were performed. Increase in anisotropy in normal and malignant tumors were observed.

A theoretical model to obtain the variation of fluorescence intrinsic anisotropy with thickness of turbid medium was based on previous reports, is developed. Validity of the model developed has been checked in tissue phantoms with a Polystyrene microspheres (dia 0.6 μm) as scatterers and FAD (Flavin adenine dinucleotide) as fluorophore.

There are three major reasons for depolarization of fluorescence, the rotational motions, the energy transfer and the multiple scattering. By eliminating effects of multiple scattering, intrinsic properties of fluorophores in different tissue environment has been obtained preliminary studies have shown that the fluorescence intensities and depolarization effects are different in normal and diseased tissues Experiments have been performed to investigate the effects of these factors In tissues and also in tissue phantom.

ACKNOWLEDGEMENTS

I would like to take this as an opportunity to express my deepest gratitude to my thesis supervisor Dr. A.Pradhan for introducing me to this exciting field of biomedical applications of laser and for her immense patience, invaluable guidance, deep involvement, stimulating discussions and constant encouragement throughtout the course of the work.

With pleasure I thank Dr. A.Agarwal and Dr. A. Rastogi, G.S.V.M. Medical college, Kanpur for their valuable suggestions and for providing the biological samples used in the present study.

Special thanks are due to Nirmalya for his deep involvement and valuable suggestions and discussions which was a great help carrying out this work

I also acknowledge the immense co-operation and big help to me in providing necessary assistance, cooperation and lively company at all time that I received from my lab mates, Ravijee, Sharad, Anoop and Shiv Kumar. Special thanks are also due to Mayajee for her wholehearted support and help during the experiments and analysis of data. I could also like to thank Chandu for his constant discussions.

Next I would like to thank my friends Atul and Arvind for their encouragement, special thanks are also due to uncle and aunty for there care and constant encouragement and homely atmosphere during the stay in IIT Kanpur.

I express my profound regards to my parents who have been a constant source of inspiration through out my carrier. It is pleasure to thank my brothers for their love, affection, help, constant moral support and active assistance during many phases of life.

List of Figures

List of Tables.

CHAPTER 1

1.1 *INTRODUCTION*

Lasers used in medicine and biology have many applications. Historically, the thermal effects of lasers have been mostly of importance especially in therapy. In recent times, laser spectroscopy plays a dominant role in number of applications. Lasers are well known in surgery as effective cutting tools. The penetration depth of laser light in tissue is largely determined by the absorption properties of water, hemoglobin, and skin pigment melanin.

Although spectroscopic aspects in terms of absorption properties do play a role in photothermal and photoablative treatment, laser spectroscopy is much more important in the fields of laser photodynamic therapy and tissue diagnostics using laser induced fluorescence (LIF). LIF studies are performed in a regime where no change in the tissue is induced by lasers. It is proven to be useful for diagnostic purpose [1].

On absorption of electromagnetic radiation, the pathways of a molecule back to the ground state are affected by its inherent structure and the physiochemical properties of its local environment. The pathways back to the ground state involve emission of electromagnetic radiation and when this emission is from a singlet state the process is called fluorescence. Fluorescence is unique among spectroscopic technique because it is multidimensional [2]. The emission process contains a wealth of information that is related to the fluorescence and its surrounding. Several groups have been investigating the use of fluorescence spectroscopy for possible cancer diagnosis and promising results have been achieved [3-6]. There exists considerable interest in the use of laser induced fluorescence from native tissues for discriminating cancerous and precancerous tissues from benign tumors and normal tissues [7]. This is because of sensitivity of this process and the time scales in which this occurs.

A brief description of fluorescence follows:

1.2 *Fluorescence:*

Luminescence is the emission of photons from electronically excited states, and can be classified by means of energy supplied to excite the molecules. When molecules are excited by interaction with photons and return to ground state by emission, the process is called photoluminescence. In fluorescence spectroscopy, molecules are excited to an activated state and undergo subsequent relaxation by a non-radiative decay and then to ground state or by a decay which results in a fluorescent photon with a lifetime of 10^{-12} – 10^{-9} seconds. A wide range of molecular processes can occur during this time period and these are reflected in the spectral profile of the fluoresing compound. Hence it is being increasly used in biomedical and chemical research. The absorption and emission of light by the energy level diagram is shown in figure1.

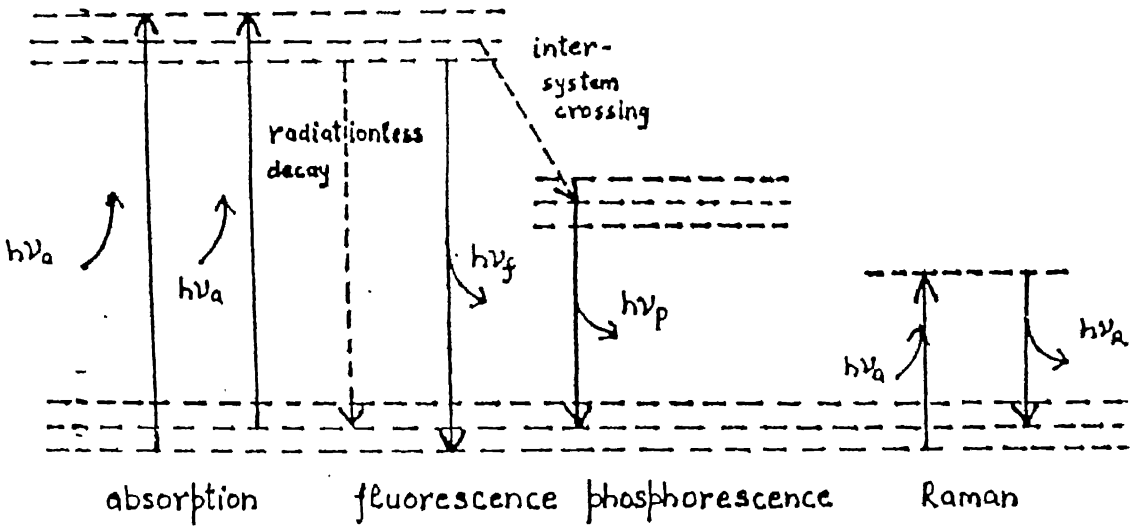

Figure 1.1: The energy diagram for the electronic and vibrational energy trasitions associated with absorption, fluorescence , phosphorescence and Raman spectroscopies.

The key parameters in the study of fluorescence spectra are: λ_{em} – the position of maximum emission intensity, λ_{ex}- the excitation wavelength, φ- the quantum yield and τ_f- the fluorescence relaxation time. These parameters are very sensitive to change in the environment of the fluorophore, and specifically in tissues, in this study. For example, an increase in the cell density of the tissue causes more non-radiative losses and due to this effect, emission lifetimes will change.

Fluorescence can be divided into static and dynamic forms. These categories can be further divided into sub categories with different features.

Static fluorescence

1) in static spectroscopy , the intensity of the profile tells us about the concentration of molecules or fluorophores , quenching of fluorophores due to molecular accessibility conformational changes.

2) The spectral profiles gives the information on the local environment surrounding the fluorophores (e.g. polarity, pH) number of emitting components.

3) The polarization or anisotropy measurements tell about the average size of a rotationally mobile species, mobility or motional restriction, binding of molecule, density of molecules.

The tools used may be

a) **Steady state fluorescence spectroscopy**:

Steady state fluorescence spectroscopy is a useful tool to diagnose biological samples, where the excitation wavelength is fixed and the emission wavelength is scanned to obtain a fluorescence spectrum.

b) **Excitation fluorescence spectroscopy:-**

Excitation spectroscopy is a useful tool to investigate medical and biological samples to identify the emitting species. The excitation spectrum is determined from the measurement of the intensities at a selected fluorescence wavelength as a function of the excitation wavelength and in general follows the absorption curve.

c) **Synchronous spectroscopy:-**

Here the excitation and emission wavelengths are both varied. The spectrum obtained is basically a convolution of absorption and emission spectra of the

sample. This method gives higher resolution as compared to other spectroscopy methods.

Dynamic or time resolved fluorescence:

1) Excited state intensity decay tells about the contribution of the individual emissive centers, continuous life time distributions.

2) Decay of anisotropy provides additional information about the diffusive motions of the fluorophore, rotational motion (i.e., if the environment is restricts its angular displacements).

Tool used is

Time resolved fluorescence

Samples are excited by an optical pulse, which is much shorter than the lifetime of the excited state of the samples. The fluorescence intensities at different wavelengths can be measured as a function of time.

1.3 *Advantages of fluorescence:*

Fluorescence spectroscopy provides a powerful method for investigating the dynamic properties of solution or molecule. This is primarily because of the lifetime of excited states. Moreover, fluorescence spectroscopic parameters are sensitive to all processes which occur during the excited state life times, and these processes can in turn affect the molecules which are $100A^0$ away from the fluorophore at the moment of excitation [2], even though 10ns seems to bea brief time span, it is a long time relative to the motions of small molecules. The rotational diffusion of proteins and membrane-bond fluorophores also occurs on this time scales. The fluorescence spectroscopy leads to large range of analysis that can be done on the profiles. It has good specificity about the environment of the molecule attached to.

1.4 *Limitation:*

Because of its sensitivity of environment it is mostly affected by the temperature, pH, and ionic strength etc, which is the major disadvantage. Quenching is another serious problem, but the analysis of various quenching processes may provide important information about the dynamics of collision between the fluorophores. These are several types of quenching observed in luminescence that is temperature, oxygen, concentration and impurity quenching.

1.5 *Biological tissue: -*

Tissue is a group of cells organized to perform a specialized function. Understanding the propagation and the distribution of light in biological tissues is important for safe use in medical diagnostics [9]. Biological tissue is optically turbid medium and normally contain several compounds, such as flavins, nucleotides (NADH), tryptophane, tyrosine, elastine, collagen etc. [8]. Flavins are intrinsic fluorophores emitting in visible region. Flavin adenine dinucleotide [FAD], flavin mononucleotide [FMN] and free riboflavin are the three forms of riboflavins encountered in biological materials. These flavins may be attached to proteins or may be free. These are coenzymes that play a role in oxidation-reduction process of the tissues. Hence, they may play a major role in triggering tumor growth [10].

Diseased tissues differ from normal tissues morphologically. However, disease may occur only with subtle visible changes. Cancer is a disease characterized by the uncontrolled growth and spread of abnormal body cells. The human body is made up of billions of cells. Normally, cells reproduce themselves by dividing so that growth occurs. Worn-out tissues are replaced and injuries are repaired in this manner. Occasionally, cells abnormally grow into a mass called a tumor. Some tumors are benign (non-cancerous); others are malignant or cancerous.

The growth of a benign tumor may interfere with body function, but these tumors are seldom life-threatening. Malignant tumors, on the other hand, invade and destroy normal tissue. By a process called metastasis, cells break away from a cancerous tumor and spread through the blood and lymphatic system to other parts of the body where they

form new tumors. Sometimes cancer grows and spreads rapidly. In other cases it develops and spreads slowly.

Breast Cancer

The most common type of breast cancer, ductal carcinoma, is found in the cells of the ducts. Cancer that begins in the lobes or lobules is called lobular carcinoma. Lobular carcinoma is more often found in both breasts than other types of cancer. Inflammatory breast cancer is an uncommon type of breast cancer. In this disease, the breast is warm, red, and swollen. Benign tumors are disease tissue which are non-cancerous. The benign breast disease includes fibrocystic disease, fibroadenoma, cystosarcoma phylloides and there are other benign disease. In India, the spectrum of benign breast disease also includes specific groups of infection viz. TB, filariasis, etc.[11].

1.6 *Focus of the thesis:*

The photon migration through tissue is an important photobiological study. Knowledge of optical parameters of tissue can be used very fruitfully as a diagnostic tool. Morphological and chemical changes inside tissues due to disease causes the fluorophores to fluoresce differently as compared to the normal environment. The different optical parameter also suffer changes due to these morphological changes which in turn gives rise to difference in fluorescence light energy distribution between cancerous and normal tissues. In this project attempts are made to differentiate between normal, benign and malignant tumors of human breast tissues by extracting characteristic information from fluorescence shape profiles and depolarization effects.

When samples are excited with polarized light, the emission is also polarized, but initial depolarization of the polarized excitation occurs during absorption and emission processes. Depolarization of the emission spectra can be due to many factors such as rotational diffusion, scattering events, energy transfer etc. when certain factors are eliminated, polarization or anisotropy may reveal more information on the environment. Depolarization studies of known fluorophores are presently utilized as probes to investigate their local environment. The major emphasize is flavin co-enzymes within the

tissue, which are fluorescence active with Ar-ion laser excitation. Fluorescence properties of flavins have been investigated between 500nm to 700nm.

The fluorescence intensities and depolarization effects are different in normal and diseased tissues. It is known that depolarization increases with multiple scattering [12]. Depolarization due to multiple scattering is the main factor in thick tissue chunks, to eliminate this factor a theoretical model is developed to obtain the fluorescence intrinsic anisotropy of turbid medium. Based on previous reports, where the anisotropy for single scattering been reduced by a factor 0.7 was reported, a 1D and 3D model using random walk and diffusion theories is developed in this thesis. Experiments have been carried out for tissues and tissue phantoms and a value of the intrinsic anisotropy is calculated.

Thesis Organization

Each chapter gives brief introduction about the contents in the chapter and introduces to the work under study. Chapter 1 introduces to the work of fluorescence spectroscopy studied here, and to different types of fluorescence spectroscopy. Discusses very briefly about the biological tissues and different types of breast tumors found. Chapter 2 describes the experimental set-up used for the fluorescence polarization studies. In chapter 3 the polarization study is carried out in two section, section A deal's with the anisotropy of the polarized fluorescence spectra obtained from different tissues. In section B just the polarized spectral profiles are studied. Chapter 4 contains the theoretical model developed using diffusion and random walk to calculate the intrinsic anisotropy from the anisotropy values (which contained depolarization due to multiple scattering) is presented.

1.7 *References:*

1. R.R.Alfano, B.T.Darayash, J.Cordero,P.Tomashafsky, F.W.Longo, M.A.Alfano, "Laser induced Fluorescence spectroscopy from Native cancerous and normal Tissues", IEEE Quantum Elect. **20** 1507 1984.

2. J.R.Lakowicz, Principles of fluorescence spectroscopy, 1983

3. C.C.Hoyt, R.R.Richards Kortum, B. costells, B.A.Sucks, C.Kittrell, N.B.Ratliff, J.R.Kramer and M.S.Feld, Laser surg. Med., **8**, pp.1, 1988.

4. R.R.Richards kortum, A.Mehta, G.Hayes, R.Cothren, T.Kolubayer, C.Kittrel, N.B.Ratliff, , J.R.Kramer and M.S.Feld, Amer.Heart J., **118**, pp.381, 1989.

5. R.Alfano, B.B.Das, E.Celmer, R.Prudente, J.Cleary, "Light sheds light on cancer-distinguishing malignant tumors from benign tissues and tumors, Bull. N. Y. Acad. Med., **67**, pp. 143, 1991.

6. G.C.Tang, A.Pradhan, W.L.Sha, J.Chen, C.H.Liu, S.J.Wahl and R.R.Alfano, "Pulsed and cw laser fluorescence spectroscopy from cancer and chemically treated normal breast and lung tissues", Appl.Opt., **28**, pp.2337, 1990.

7. R. Richards -Kortum R and Sevick-Muraca E.,"Quantitavive optical Spectroscopy for tissue Diagnosis", Annu. Rev. Phys. Chem., **47**, 555-606, 1996.

8. A.Pradhan ," Fluorescence Spectroscopic properties of Normal and Abnormal Biomedical materials", Thesis City University of New York,1991.

9. M.S.Patterson, B.C.wilson and D.R.Wyman," The Propagation of Optical Radiation in tissues", Laser Med. Sci.,**6**,155 , 1991.

10. S.Ghisla, V.Massey, J.Lhoste and S.G.Mayhew," Fluorescence and Optical Characteristics of reduced Flavins and Flavoproteins", Bio-Chem., **13**, 589, 1974.

11. A.Rastogi,"Evaluation of various Diagnostics Modalities in Breast Lesions with special reference to role of Laser Spectroscopy", Thesis in S.S.M.Kanpur University, 2000.

12. L.W.Teale, " Fluorescence depolarizatin by light- scattering in turbid solutions", Photoche. Photobiol. **10**, 463, 1969.

Chapter 2

2.1 *Introduction*

The successful application of a spectroscopic method requires an understanding of its instruments. Considerable attention to the experimental details is therefore necessary. In this chapter the experimental set up for the emission spectra is described in detail.

Absorption and emission polarization spectroscopy has served as useful tools for identifying fluorophore electronic states and conformational structure in different environments. The harmful effects of X-rays and nuclear radiation have forced scientists to resort to other techniques such as Ultrasonography, immune diagnosis computed tomography and imaging tissues. Fluorescence spectroscopy is a recent development in this category growing very fast[1].

The description of the instrumentation involved in the photoluminescence spectroscopic measurement is described here. The essential instruments in used are Argon ion laser, the chiller plant, the spectrometer and the photomultiplier tube (PMT) constituting the spectroscopic measurement set up, is briefly described in this chapter.

2.2 *Experimental Set-up for fluorescence depolarization* :

The block diagram of the experimental set up used for the measurement of steady state fluorescence polarization[2] from normal and tumor human breast tissues has been shown in figure 2.1. The samples were excited with linearly polarized argon-ion laser light operated at 488nm with ~2mw power at the sample site (power at source is 100mw). Any fluctuation in laser power was less than 0.3%. The linearly polarized light was focussed onto a spot size of nearly 10μm on the front surface of the tissue. The

fluorescence light from the front surface of the tissue was passed through an analyzer whose optic axis was set parallel or perpendicular to the optic axis of the polarizer. A depolarizer was placed before the spectrometer to ensure that the detection

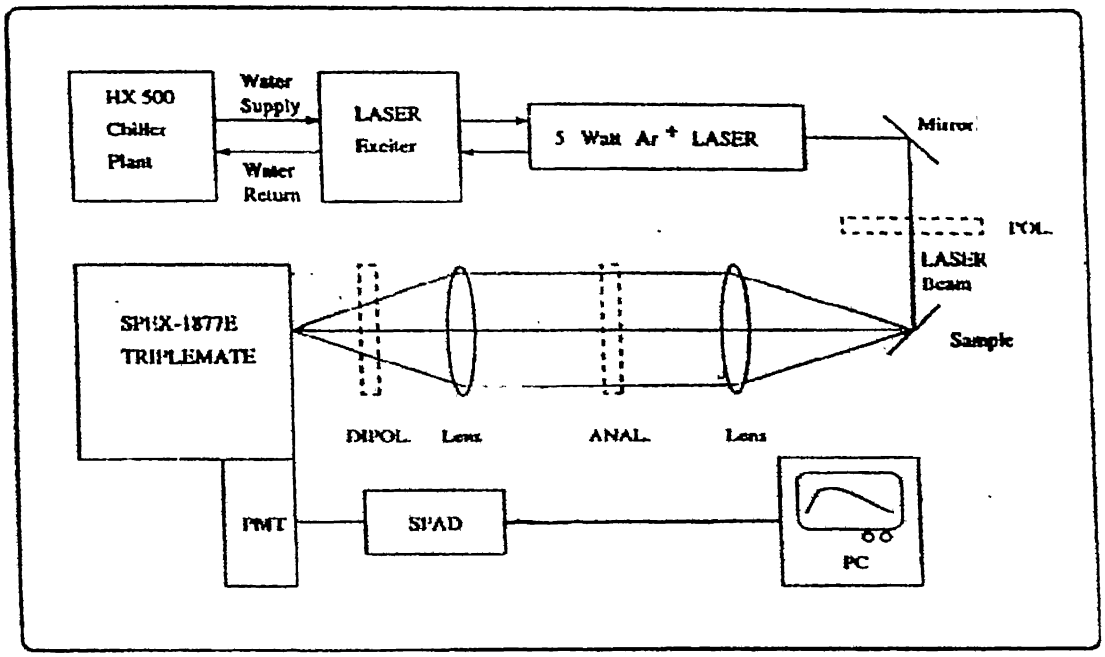

Figure2.1: Schematic diagram of the steady state fluorescence polarization apparatus.

system does not give preference to any one of the selected directions of polarized luminescence . The fluorescence is recorded using a SPEX-1877 E triplemate blazed at 500nm and cooled photomultiplier tube (PMT). The output of the detector was connected to computer for data acquisition and analysis.

5 Watt Ar-ion Laser

Spectra physics model 165 Ar-ion laser mainly consists of a laser head and 265 exciter. With a start boost circuit(by 7Kv pulse) , the exciter generates an initial start in the plasma tube. This exciter also contains a regular power supply that controls the ion-discharge current in the plasma tube to provide constant laser performance. The laser head consists of a plasma tube of Berylium oxide (both ends are closed by Browster

angle windows) , a solenoid and an optical resonator. The resonator consists of a spherical mirror at the output end and a prism assisted a flat mirror at the back end.

Cooling system for Ar-ion laser:

Ar-ion laser requires cooling for the transistor pass bank in the exciter, magnetic field solenoid and the plasma tube. The Neslab chiller plants have been used for the cooling. The chiller plant mainly consists a reservoir, temperature controller, re-circulating pump, a refrigeration unit. This chiller plant provides continuous flow of sufficiently deionized water at constant temperature and pressure in a closed loop of external apparatus. It supplies a continuous flow of water (20°C) and pressure of 31psi to the laser head. The cooling capacity of this plant is 15.7 kw.

Spectrometer (SPEX 1877-triplemate)

The SPEX 1877 –triplemate is a spectrograph specially tailored to provide low stray light and flat undistorted focal plane, ideal for sensitive work with optical multi-channel detector. The optical path of the triplemate is shown in figure 2.2.The collected scattered radiation passes through the entrance of filter stage to collimated by mirrors M1 onto grating G1 (600 grooves per mm) where it is dispersed into focussing mirror F1. After passing through S2 , which determines the band pass of the filter state, the light strikes spatial filter mirror (SF) and passes through a torroidal lens and a fixed slit (S3) which illuminates much of the stray light .Again the light is collimated (M2) dispersed G2 (600 grooves per mm) in an opposite direction to cancel the effect of initial dispersion, then focussed (F2) into the exit slit S4 of the filter stage, which determines the resolution of spectrograph stage. The flight is again collimated (M3) and dispersed by the grating G3 (1200 grooves per mm).

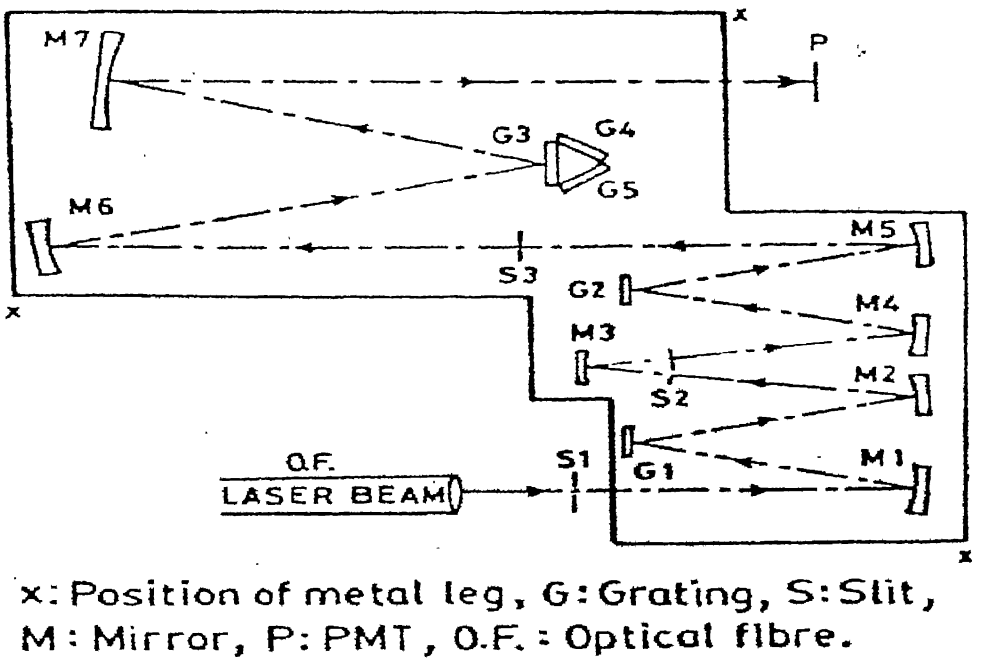

Figure 2.2 optical path of triplemate Spectrometer.

Photomultiplier tube(PMT)

The PMT is a photosensitive device consisting of a photo-emissive cathode followed by focussing electrodes, and electron multiplier and a electron collector in a vacuum tube. The photo- cathode emits photo electrons when light falls on it. These are then directed by the focussing electrode voltages towards the electron multiplier where electrons are multiplied by the process of secondary emission. The multiplied electrons are collected by the anode as an output signal. By operating the PMT at –30°C using the Peltier effect dark current, the effects are minimized so as to allow measurements of weak signals. It takes nearly 90 minutes (after switching on to attain this temperature).

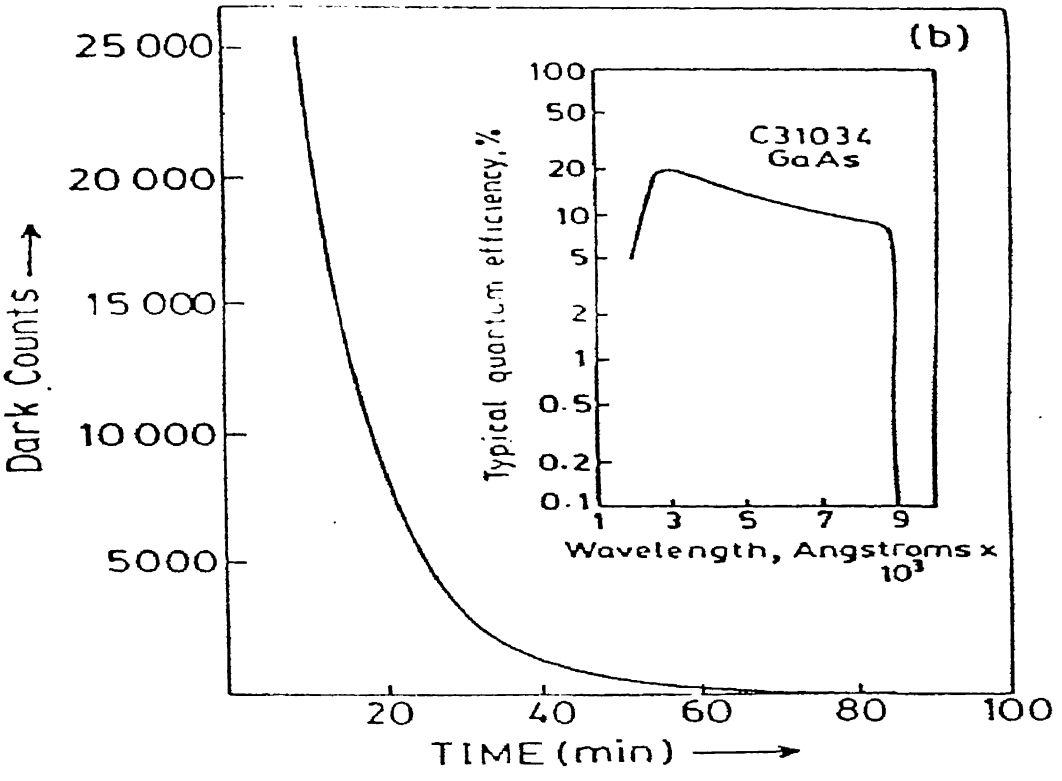

2.3 Dark current-vs-time curve after switching on the thermoelectric cooling of PMT. The inset shows quantum efficiency of PMT with wavelength.

2.3 *References:*

1. Fluorescence Diagnosis and photochemical treatment of diseased tissue using Laser - Part I, Analytical Chemistry, Vol. 62, No.1, Dec. 15 1989.

2. Manish purwar, " Studies of fluorescence Depolarization and spatial dependence of scattering using optical fibers in human tissues", CELT, IITkanpur, 1997.

Chapter 3

3.1 *Introduction*

Absorption and emission polarization spectroscopy serves as useful tools to probe the environment of the fluorophores. It is established that the polarized spectroscopic properties of the fluorophores are highly dependent on polarity, pH and viscosity [2]. Depolarization studies of known fluorophores are utilized as probes to investigate their local environment. In tissues, which are the samples used in this study, there are several proteins, enzymes, etc that fluoresce. There are known protein bound fluorophores within the cells such as flavins that fluoresce in the visible range. Flavins are important in oxidation-reduction processes, which may play significant role in progress of disease due to change in environment of flavins or flexibility of flavin-protein binding.

Visible fluorescence spectroscopy has not shown very significant results. Researches have concentrated more on UV excitation of tissues. Our aim is to use fluorescence depolarization to probe in more details in visible region for any distinguishing features and more information on the environment of flavins. The size shape or segmental flexibility of the fluorescence can also be probed by fluorescence depolarization measurements. 488nm excitation has been used for the study of flavin environment. In this chapter a detail study of the spectral profiles and depolarization of human breast tissues has been presented.

When samples are excited with polarized light, the emission is also polarized. This is a result of the photoselection of fluophores, which are oriented in the direction of the polarized excitation. Initial depolarization occurs during absorption and emission processes. Because electric dipole of a fluorophore need not be precisely aligned with the Z axis to absorb light polarized along this axis, the probability of absorption is proportional to the $\cos^2\theta$, where θ is the angle between absorption dipole and Z axis. Hence the excited state contains fluorophores which are symmetrically distributed around

z axis, this phenomenon is called photoselection. Hence fluorescence is not totally polarized. During emission, depolarization of the emission spectra can be due to many factors such as rotational diffusion, scattering events occurring, energy transfer etc. When certain factors are eliminated, the polarization or anisotropy measurements may reveal the average angular displacement of the fluorophores which occur between absorption and subsequent emission of photon [1]. Alfano and co. workers studied fluorescence polarization spectra in Rat tissues[3], in which they got high polarization for normal compared to malignant tissues. They reported that relaxation time, $T_{rot\ normal}$=808ps and $T_{rotcancer}$ =117ps, this indicates that the flavin fluorophores are more loosely bound to the enzyme and proteins within the intercellular environment of the cancerous cells. Hence rotational depolarization in cancer is more.

3.2 *Definition :*

Anisotropy and polarization:

When the sample is excited with vertically polarized light, the measured intensity of the emission parallel to direction of the polarized excitation is $I_{||}$, and the intensity perpendicular to initial excitation is $I_{\perp}$ as shown in figure3.1.

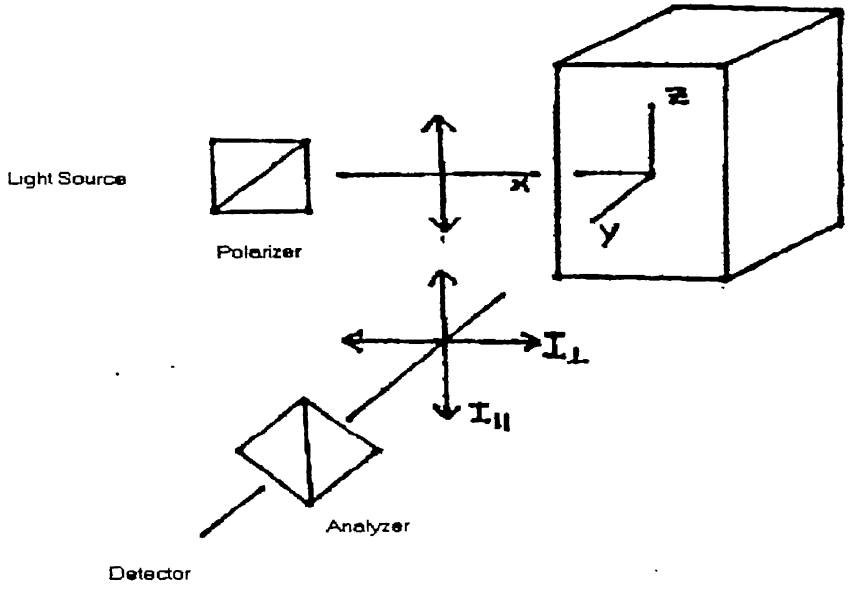

Figure 3.1: Schematic diagram for measurement of fluorescence anisotropy.

Polarization is defined as :- $(I_{II} - I_{\perp})/(I_{II} + I_{\perp})$ (1)

Anisotropy is:- $(I_{II} - I_{\perp})/(I_{II} + 2I_{\perp})$ (2)

For completely polarized light $I_{\perp}=0$, which implies that P= r =1, which is for scattered light, fluorescence emission is symmetrically distributed about the z-axis. Hence, the anisotropy is the ratio of the excess intensity, which is parallel to the z axis to total intensity. Therefore, anisotropy is used for fluorescence steady[1].

3.3 *Experimental Method:*

Pathologically characterized thick (~4mm) tissue samples were obtained immediately after surgery. The experiments were done on the same day of operation, without any chemical treatment. Most of the tumor tissues studied were ductal carcinomas. The benign tumors were of different types. The normal tissues were from the surrounding areas of the resected cancerous tissues.

The experimental setup used for fluorescence depolarization is shown in Figure 2.1 of chapter 2. The parallel and perpendicular intensity components of the

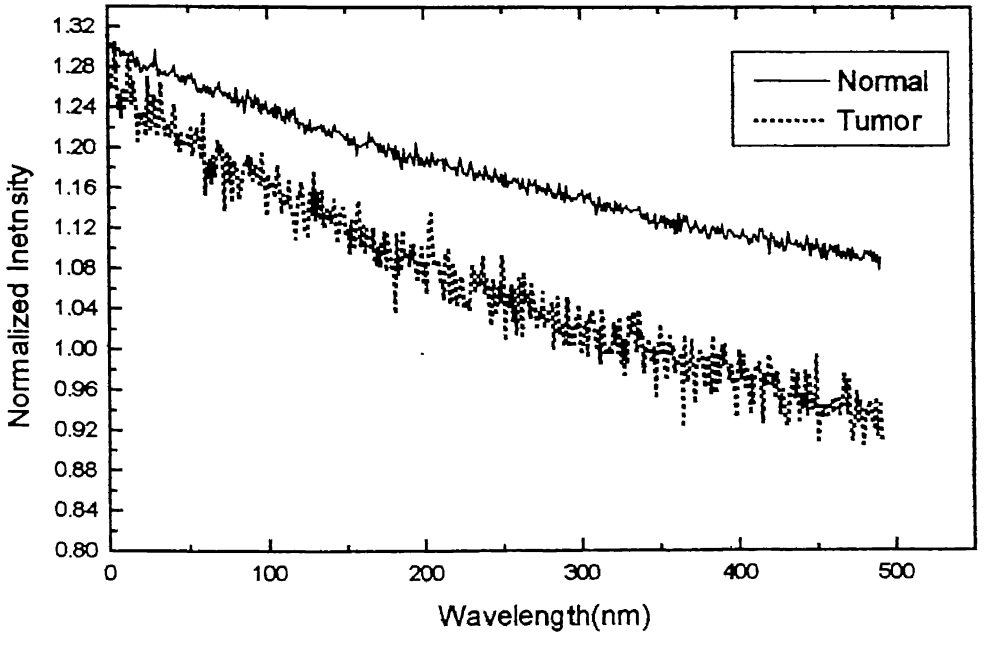

Figure3.2:The photobleaching curves for both the types of human breast tissues (Normal and Malignant).

luminescence for each sample were scanned separately and the anisotropy was calculated using the relation defined above. The fluorescence depolarization data were obtained from malignant tumor, benign tumor and the normal breast tissues. All the anisotropy observation were done in steady state i.e. by bleaching the samples for 15 to 20min, to minimise the photo-bleaching effects due to laser radiation. Figure 3.2 shows the bleaching curve for both normal and tumor tissues. For measurements, samples were placed in optical cuvettes of $1\times1\times5cm^2$. Samples were in the form of thick and thin slices of thickness 4mm to 0.5mm respectively.

3.4 *Results and Discussion:*

Section A

Normalized fluorescence spectral profiles from normal, benign and malignant human breast tissues excited at 488nm along with the fluorescence spectra of flavin adenine dinucleotide (FAD) are shown in Figure 3.3. All the spectral profiles have main peak centered around 530nm, which is attributed to flavins, as flavins are natural fluorophores present within intact cells that emit in the visible region 510-550nm[4]. The profiles of normal and tumor are similar to but broader than that observed for aqueous solution of (1.0×10^{-4}M) FAD, which may be due to the following factors. The fluorescence peak centered ~530nm is known to be mainly from flavins, e.g., flavin adenine dinucleotide, flavin mononucleotide and free riboflavin. It is known from literature that the dinucleotide accounts in for 70-90% of the total riboflavin content. FAD has a fluoresence equal to 15% of riboflavin in tissue where as FMN and riboflavin fluoresce in equal amounts. Therefore, the fluorescence emitted from such tissues is mainly due to various forms of flavin mononucleotide. Further, the peak position and intensity are found to vary in flavoproteins due to formation of complexes with other molecules, e.g. tyrosine or tryptophan, presence of hydrogen bridge between protein and

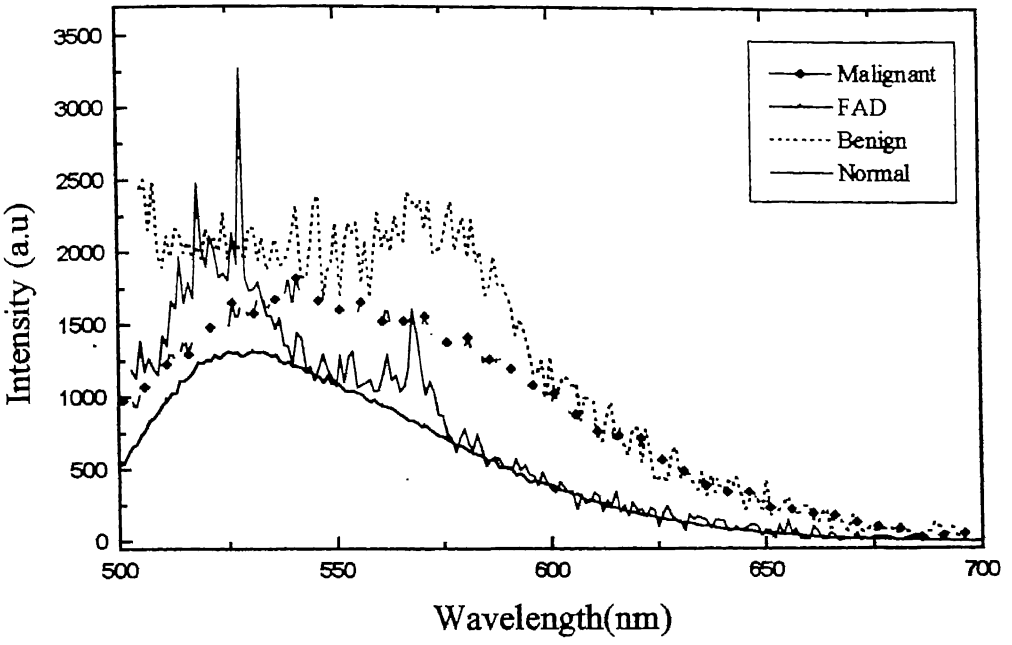

Figure 3.3: Fluorescence spectral profiles for a) Malignant breast tissue, b) aqueous solution of FAD, c) Benign breast tissue, d) Normal breast tissue.

coenzyme [9].

Normal tissues were of two different types, one yellowish and fatty and the other more fibrous and less yellow. The fatty tissues always showed Raman peaks at 1148.9, 1520.4 and 2891.8 cm^{-1}, as reported earlier [5], but peaks at different positions compared to the earlier results. In almost all the normal tissue spectra a secondary band was observed at 560±5nm. Even though all the samples were cleaned in saline to remove blood from tissues, there was some blood in the normal samples. Therefore, the second band could be due to blood (oxyhemoglobin) absorption, which is reported to be at 540nm[4]. The main peak in normal samples were at 525±5nm, average fluorescence spectra of 40 curves each of normal breast tissues is shown in Figure 3.4

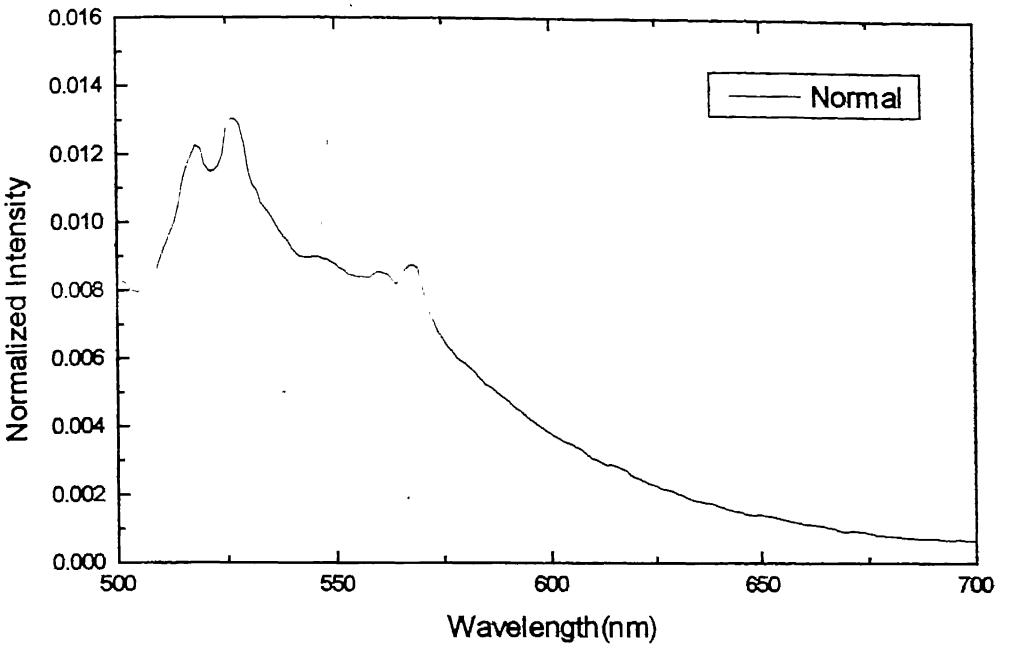

Figure 3.4: The average Fluorescence spectral profile for all normal human breast studied.

Similarly Figure 3.5 displays the average fluorescence spectra of 18 malignant samples, which shows the monotonous decrease in intensity without any secondary peak. In benign tumors the wavelength band at 580nm remarkably prominent and fluorescence profiles appeared to be broadened, which may be due to other fluorophores present. Average fluorescence spectra of 22 benign samples is shown in figure 3.6. The results of benign tumors are discussed in detail in the next section.

Figure 3.7 and 3.8 shows the polarized fluorescence spectra of normal and tumor tissues. In each of these figures the parallel ($I_{\parallel}$) and perpendicular ($I_{\perp}$) profiles are recorded only in steady state conditions, in which the bleaching effects are minimized to 4–5%, such that the reduction is with in the noise margin of the detector. As shown in Figure 3.2 bleaching in tumor is fast compared to normal, which implies that if anisotropy is calculated with unbleached fluorescence spectral profiles, this will always result in higher anisotropy for tumors. To minimize this artifact, measurements were

taken at steady state. For further confirmation, perpendicular component and then the parallel components were recorded and no change in anisotropy was observed.

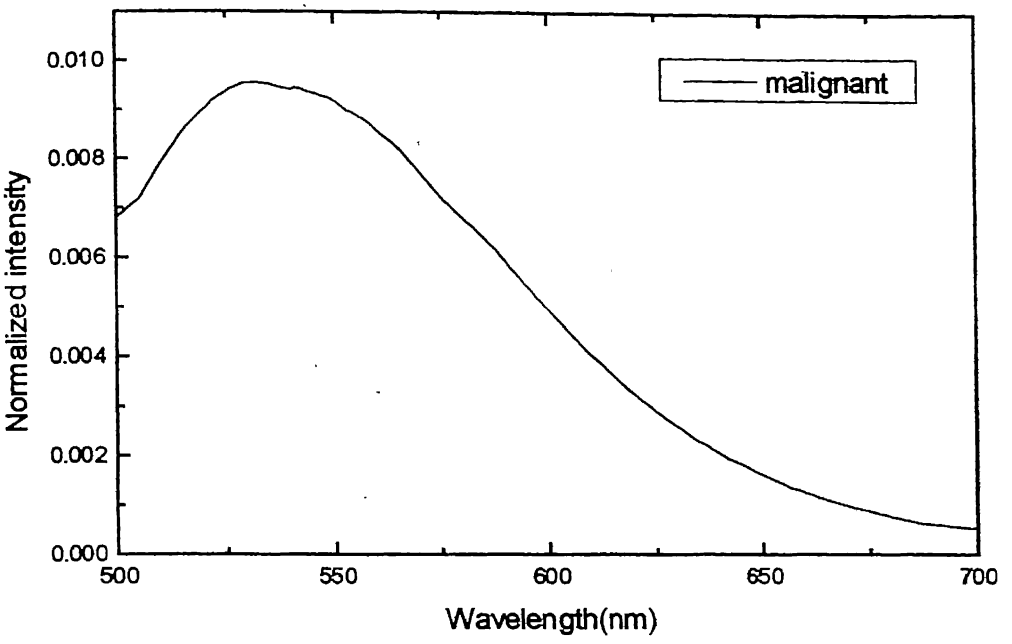

Figure 3.5: The average fluorescence profile of all malignant cases studied.

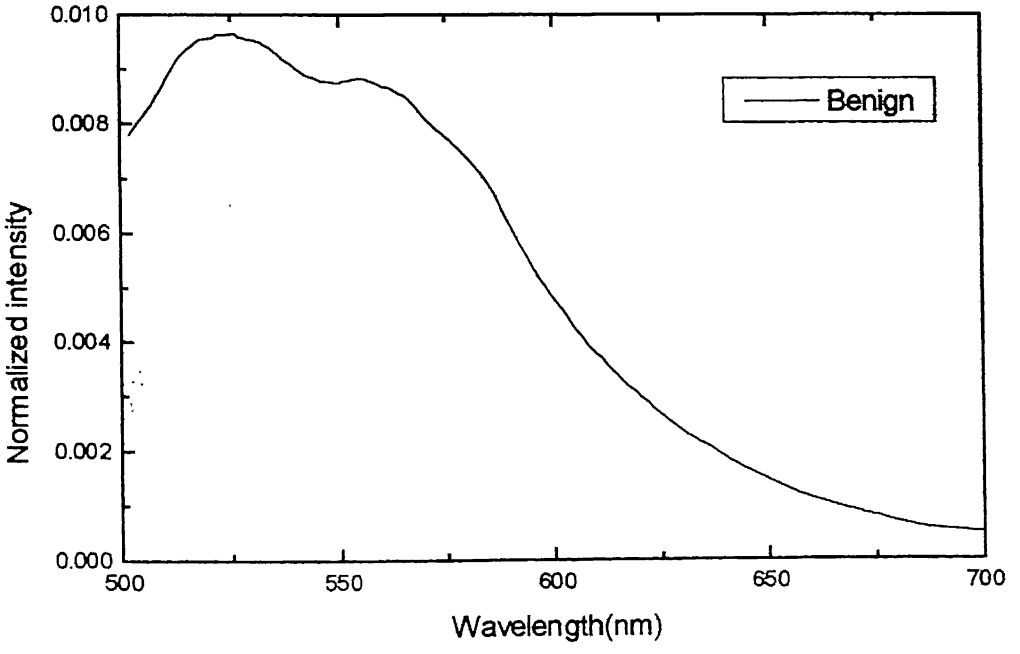

Figure 3.6: The average fluorescence spectral profiles of all benign cases studied.

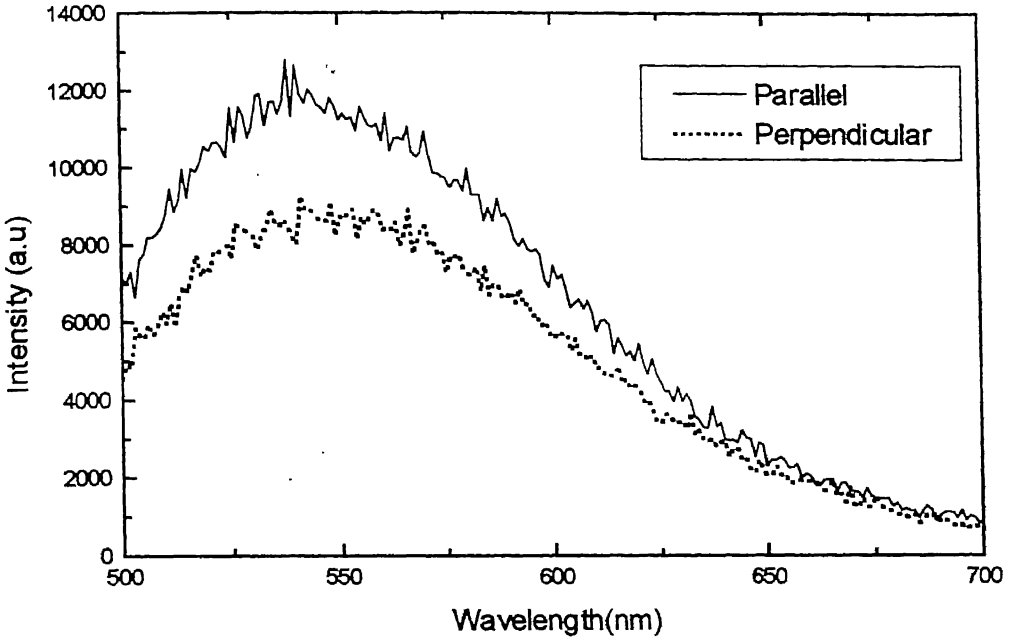

Figure 3.7: Polarized spectra for malignant breast tissue.

Photo-bleaching is a dynamic process in which fluorophore molecules undergo photo-induced chemical destruction upon exposure to excitation light and thus loss their ability to fluoresce. The rate of photo-bleaching is a function of the excitation intensity. However, the mechanism of photo-bleaching in biological objects are not yet well understood due to the complexity of the heterogeneous fluorophores and the chemical environments attached to fluorophore molecule [6].

Bleaching of the samples can be due to different processes occurring in the tissue by laser excitation, for example photochemical reaction, diffusion of the molecule to other regions or quenching of the fluorophores etc.. While recording the fluorescence spectra for anisotropy calculation in our system, these processes have been minimised by exciting the samples with low power and by recording the time base scan (i.e. to observe the intensity variation at a particular wavelength here 530nm with time).

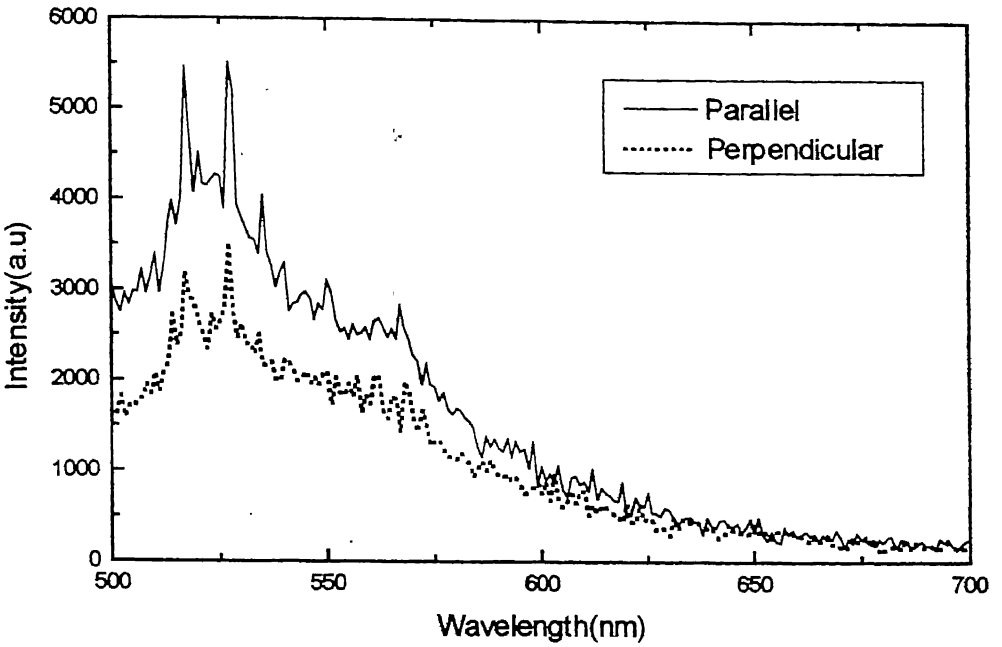

Figure3.8: Polarized spectra for normal human breast tissue.

Out of 40 cases studied, 21 cases were showing higher anisotropy for tumor breast tissues, and 10 cases showed opposite results. In remaining 5 cases, 4 cases does not had the normal counterpart even though for these cases the anisotropy for tumor tissues was high (~ 0.08 to 0.17), but as the anisotropy depends on environment effects which differ from tissue to tissues, hence they were not considered. Remaining case had both the tissue from infected area. The anisotropy values were obtained by fitting the fluorescence profiles(parallel and perpendicular) to voigt functions and using the 530nm band intensity in equation 3.1. Statistics of the results for 35 samples is shown in table 1.

Cancer	No. of Samples	31
	Sensitivity	71.4
	False negative	28
Normal	No. of Samples	31
	Specificity	71.4
	False Positive	28

$$\text{Sensitivity: Percentage of cancer detection in agreement with pathologists} = 100\times \frac{\text{No. of correctly diagnosed cancer samples}}{\text{Total no. of cancer samples}}$$

$$\text{False negative: Percentage of cancer detection not in agreement with pathologists} = 100\times \frac{\text{No. of incorrectly diagnosed cancer samples}}{\text{Total no. of cancer samples}}$$

$$\text{Specificity: Percentage of normal detection in agreement with pathologists} = 100\times \frac{\text{No. of correctly diagnosed normal samples}}{\text{Total no. of normal samples}}$$

$$\text{False negative: Percentage of normal detection not in agreement with pathologists} = 100\times \frac{\text{No. of incorrectly diagnosed normal samples}}{\text{Total no. of normal samples}}$$

Table 1.

With this sensitivity and specificity table 2 shows mean and standard deviation of the anisotropy values for different types of tissues calculated at 530nm.

Type of tissues.	Anisotropy (530nm)
Normal	0.09±0.02
Malignant	0.148±0.02
Benign	0.19±0.043

Table2.

The salient feature of these results is higher degree of anisotropy exhibited by the (malignant and benign) tumor tissues compared to normal breast tissues. Higher degree of anisotropy of cancerous tissues means that flavins are less depolarized, that is flavins are tightly bound to the proteins. Fluorescence depolarization can occur mainly because of Brownian rotation motion of the excited fluorophores as well as energy transfer mechanisms. In earlier work, fluorophores in low and moderate viscosities at room temperature has shown that Brownian rotational motion is the main cause of depolarization in various fluorophores and not the energy transfer mechanism [3]. It is

known that depolarization of any propagation light occurs due to multiple scattering [7]. Based on this , it is expected that tumors should show a lower anisotropy as compared to normal tissues. Since tumors have more densely packed cells hence scattering will be more enhanced. However, our results show deviation from this. This may be due to the

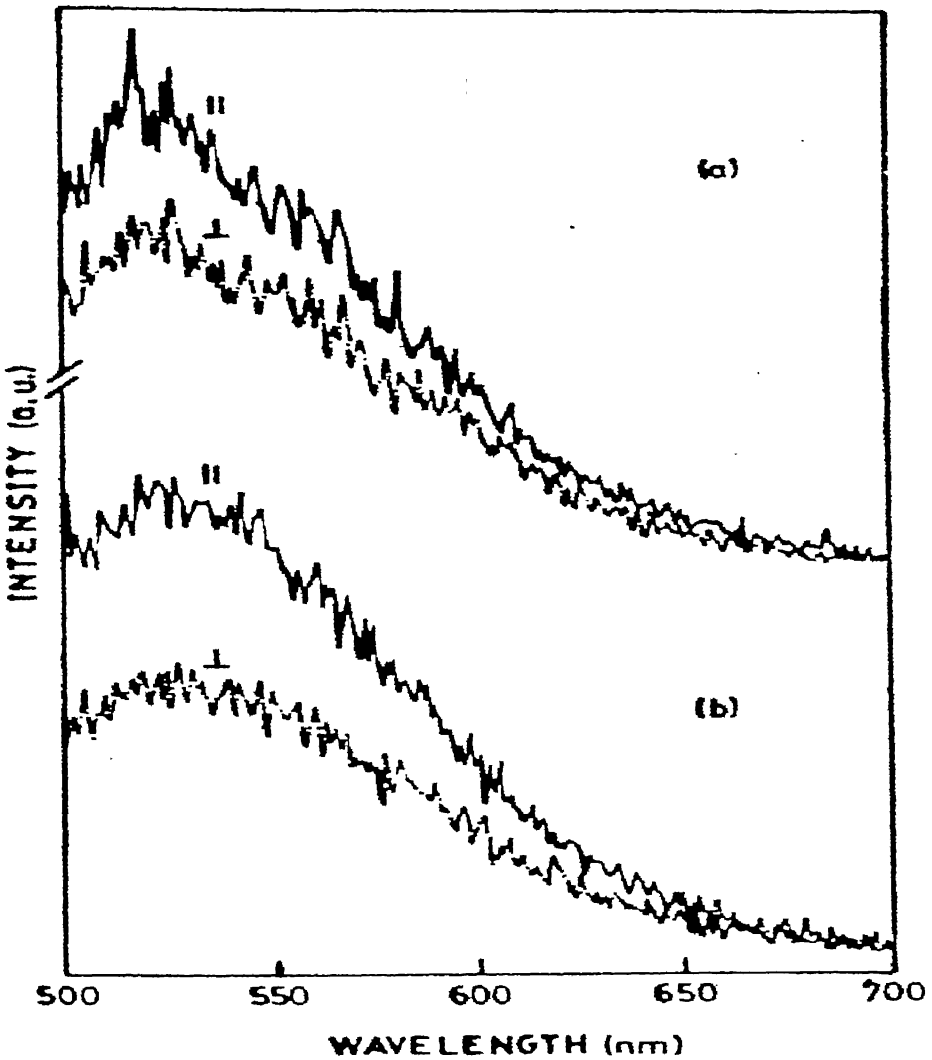

Figure3.9:Shows the polarized fluorescence spectra for both thick(a) and thin (b)tissue sections.

fact that in thick samples the scattering effects in normal and tumor are there in equal amounts and it has less contribution than other effects. And as the perpendicular

component comes into picture through scattering effects, ie, if there is large number of scattering events there will be gain in the perpendicular component. But through spectial variation experiments, we observed that absorption coefficient (μ_a) per mm at 530nm for normal is 0.07 and for malignant it is 0.16. As the perpendicular component is the one which travels longer path before it gets collected and hence gets more absorbed at 530nm, leading to larger difference in $I_{\parallel} - I_{\perp}$ [1] therefore tumor results in high anisotropy. To probe more information on it, the scattering effects experiments were done on thin tissues sections (0.5mm). The thin samples showed increase in anisotropy in both normal and tumor tissues , Figure3.9 shows the polarized fluorescence spectra for both thick and thin tissue sections.

It is interesting to note that for normal tissue, anisotropy has increased in thin tissues compared to thick (for example 0.5mm and 4mm)tissue chunks. In figure 3.9 (a) and (b), shows the thickness variation vs. anisotropy normal and tumor tissues and Figure 3.11 shows both normal and tumor anisotropies with thickness variation.

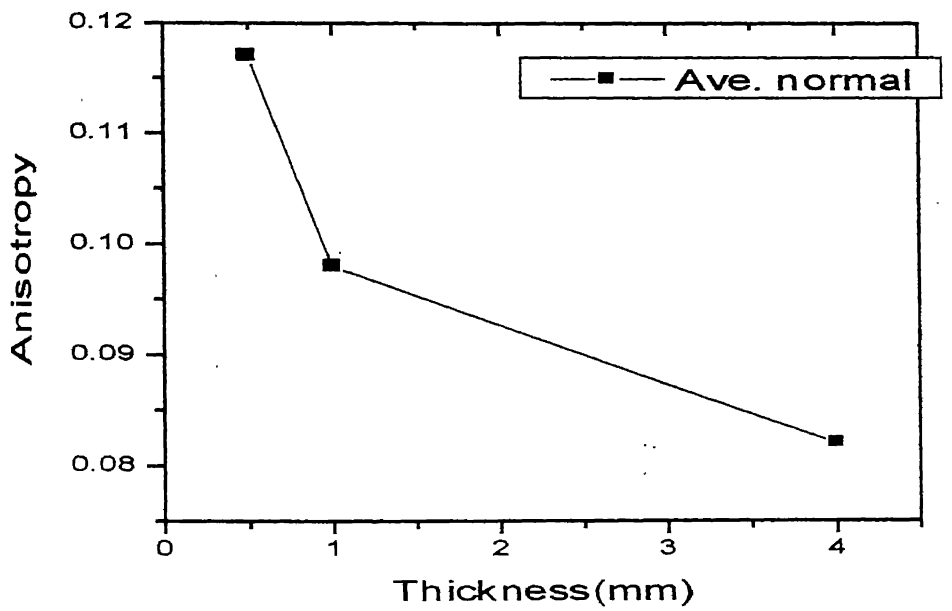

Figure 3.10 (a)

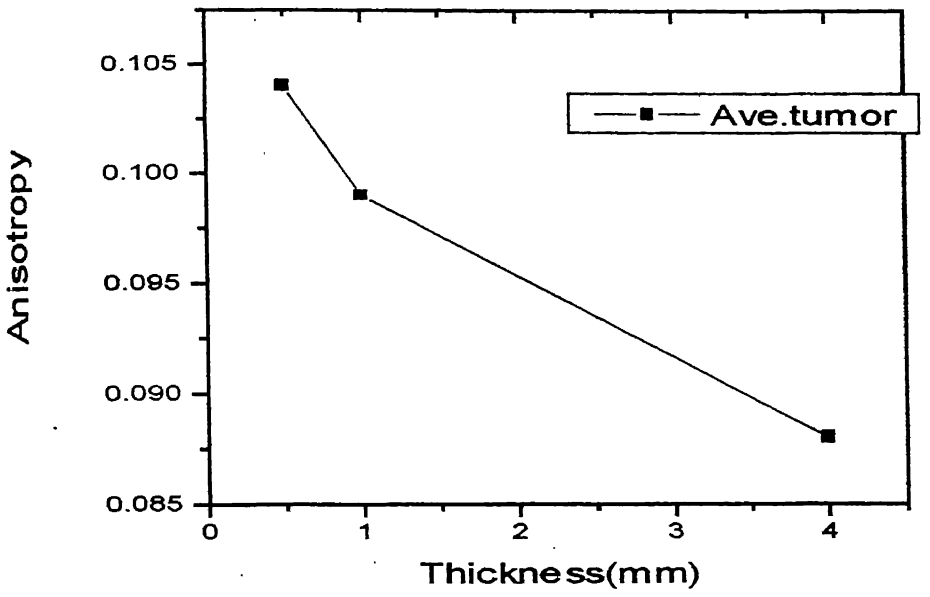

Figure 3.10: Thickness Vs. anisotropy (average of all the cases studied), a) normal breast tissue, b)tumor breast tissue..

In thick tissues (i.e., 4mm) excitation light suffers more multiple scattering in tumors. Hence depolarization effects of fluorophores may be higher in tumors. While going from thick to thin, we expect the increase in anisotropy in tumors as well as in normal tissues. Interestingly this is observed, but in some of the cases anisotropy of tumor decreased at 0.5mm compared to anisotropy observed for thickness greater than 1mm.

Absorption and scattering lengths for normal and tumor at 488nm comes out to be (from spatial variation experiments), $l_s(T)$=1.5mm $l_s(N)$=1.7mm and $l_s(T)$=0.16mm, and ls(n)=0.2mm respectively[14]. This results that at 4mm (which is the thickness very much greater than the lengths given above) the scattering in both the tissues are saturated

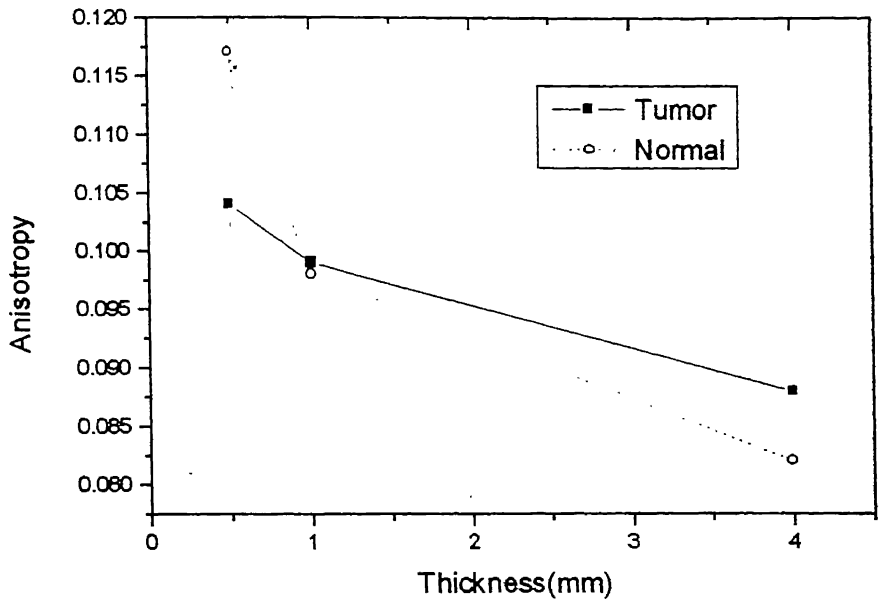

Figure 3.11: Anisotropy vs. thickness for both normal and tumor breast tissue.

and at 1mm we have minimized the scattering effects (which are more dominant in tumors). Hence observed the increase in anisotropy. Around this thickness, the absorption coefficient effects are reduced compared to thick tissues. Since l_a (absorption length) is much larger than the thickness. On the other hand scattering coefficient values show that scattering length $l_s$of 0.2mm and less, such that multiple scattering effects dominates in this region. Sice μ_s of tumor is higher that normal multiple scatetring effects are more in tumors than in normal and anisotropy of normal is higher as expected.

Figure 3.11 shows the anisotropy of average of all the cases studied, where the crossover of anisotropies for normal and tumor human breast tissue occurs. This, crossover is different for different types of tissues, for 11 cases studied here the cross over is at 1mm.

For 8 malignant cases out of 9 cases, anisotropy at 0.5mm for normal is more than tumor and for remaining malignant case anisotropy in both tissue types were nearly equal, out of 11 samples which were studied with thickness variation from 4mm to 0.5mm in steps of 1mm. Other 2 cases were of benign type, showing anisotropy of

normal to be equal to tumor ones. Concentration of the fluorophores is another factor, which affects the anisotropy [5]. In our studies with tissues, the flavin concentration may be different from sample to sample, hence may be the reason for not getting a clear cut off value of anisotropy.

3.5 Section B

3.5.1 *Introduction:*

The use of fluorescence spectroscopy is limited as a diagnostic tool because the measured spectrum is distorted by the absorption and scattering properties of tissue[8]. However, by the modeling of excitation and fluorescence light propagation, observed fluorescence can be related to intrinsic tissue fluorescence. Attempts to eliminate the effects of tissue optical properties on measured fluorescence spectra have been based on theoretical description of light propagation in a turbid medium, which produces an analytic relationship between measured and intrinsic fluorescence. Carig M. Gardner and co-worker[9] have made attempts to develop a method for recovering the intrinsic fluorescence coefficient, defined as the product of the fluorescence absorption coefficient and the fluorescence energy yield, of an optically thick homogeneous turbid medium from a surface measurement of fluorescence and from knowledge of medium optical property

As light propagates through a turbid material (such as tissue), it can be weakly scattered and travel a direct path through the material or it can be highly scattered and travel a more circuitous route through the material and get absorbed along the path of travel in both the cases. Extraction of the weakly scattered light from the highly scattered light can give better picture about the material under study.

Recently there has been considerable interest in using the polarization state of light as a discrimination criterion[10]. Weakly scattered light retains its initial polarization whereas highly scattered light gets more depolarized. The parallel component of fluorescence retains more information of intrinsic fluorescence as compared to perpendicular component. Thus, parallel component may be used to extract more information on the environment. In this section attempts have been made to extract

more information on intrinsic property of different types of tissues using very simple method.

3.5.2 *Results & Discussion:*

Figure 3.12 shows the normalized fluorescence spectra for FAD solution of 1×10^{4}M contaning parallel and perpendicular components, of polarized excitation at 488nm. Since there are no absorbers or the scatterers it is expected that for this solution which contains only fluorophores, the profiles of parallel should exactly match with the perpendicular. As explained in the introduction the perpendicular component is more effected by the scattering and absorption in the medium. And in solution with these factors are eliminated, hence the parallel and perpendicular profiles matches well as shown. Polarized fluorescence profiles of all the 40 samples studied whose anisotropy

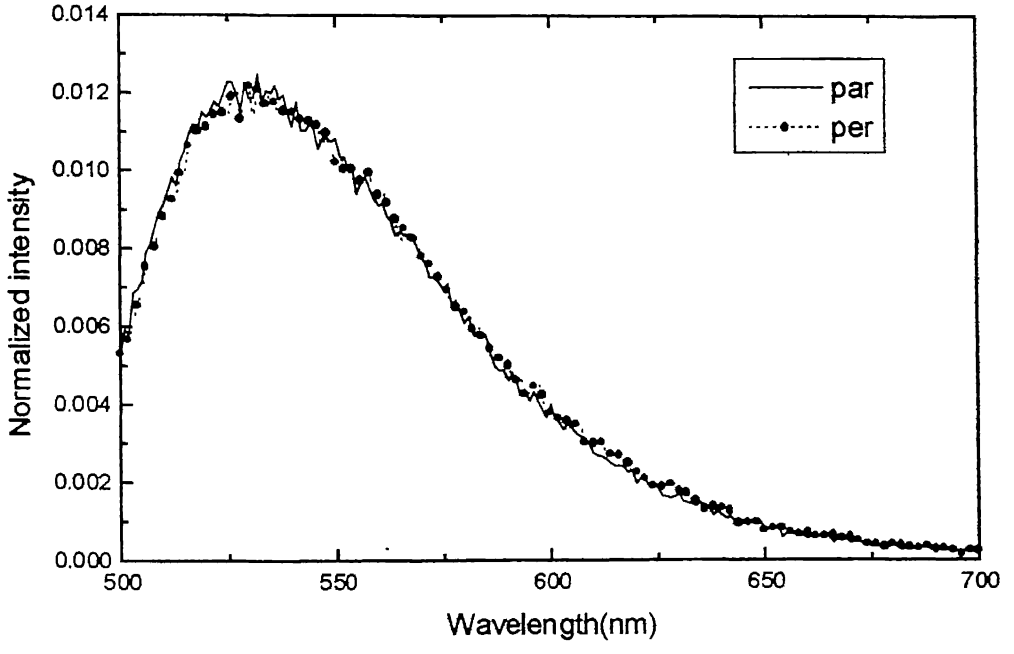

Figure 3.12:Normalized fluorescence spectral profile containing parallel and perpendicular components for FAD solution of 100μM.

has been measured, and analysed. Figure 3.13 shows the normalized fluorescence spectra of malignant human tissue(both parallel and perpendicular profiles) along the polarized spectral profile of FAD solution (1×10^{-4} M) excited with 488nm. Parallel and perpendicular profiles are the average of all the cases studied. The profiles of malignant appears to be broader which may be due to other molecules present the tissue or scattering effects may also broaden the profile. It is observed that the perpendicular component is even broader, and the intensity at 530nm is less compared to parallel profile. As discussed earlier in the introduction the perpendicular component is the one which travels longer path and hence experience larger effects of scattering and absorption. In Figure 3.14 normalized average spectra of parallel and perpendicular

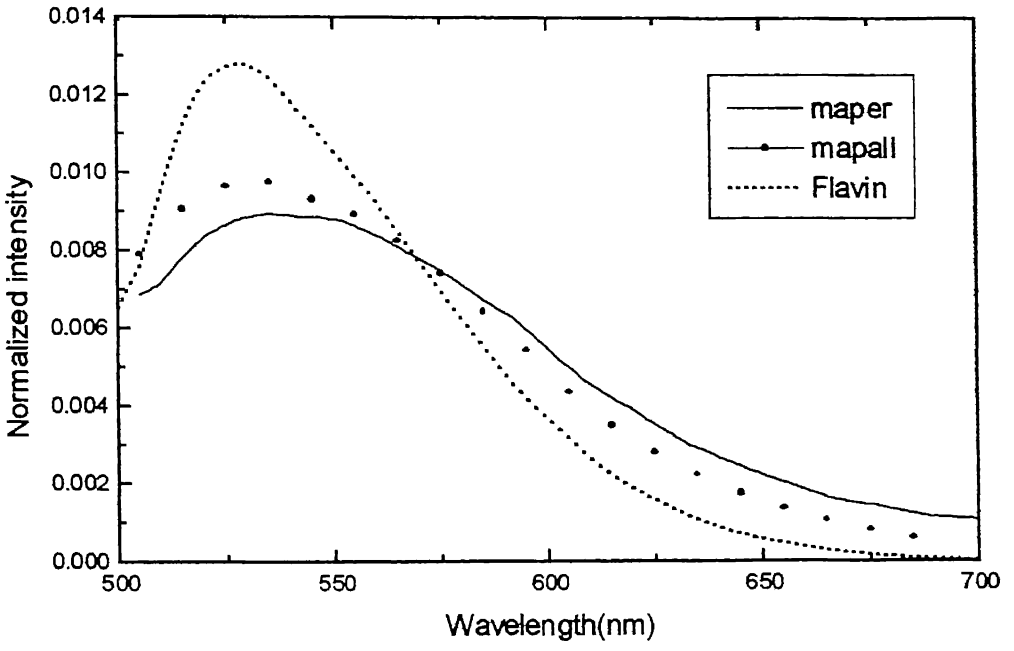

Figure 3.15: Average of parallel and perpendicular fluorescence spectra of malignant cases.

component of normal breast tissues shown, as there are less number of scattering centers, in normal tissue compared to malignant, we expect that the broadness is less here compared to malignant. This is observed, but the difference is not significant. This may be due to the fact that at thick tissues the scattering effects in both normal and malignant are saturated because l_s for normal and malignant is 0.2 and 0.16 mm respectively .

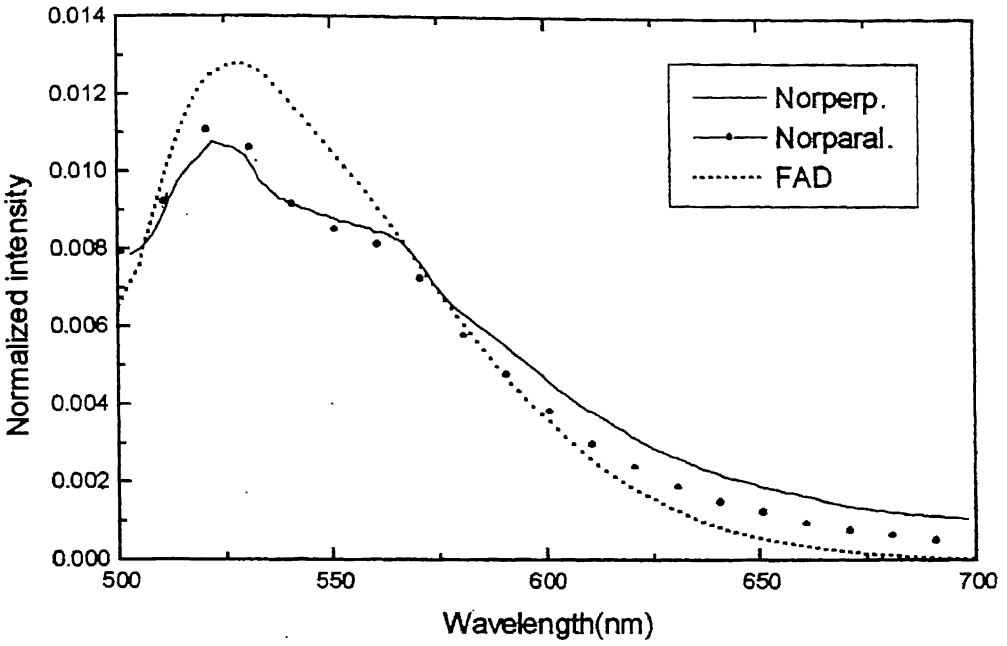

Figure 3.15: Normalized average fluorescence spectra of parallel and perpendicular of normal cases.

In thick tissues of thickness 4mm there are equal amounts of scattering occurs in both types of tissues. Table 3 displays the values of μ_a and μ_s for all 3 types of breast tissues[13].

In the case of benign, there appear to be two distinct bands. The relative intensities of both the bands are different for different samples and are well separated in some cases as shown in Figure 3.16. Hence the average of all parallel component displays a smoother profiles as compared to individual spectra. The average perpendicular component shows broad band, but the intensity at 600nm is less than that of parallel plot

Type of tissue	Value of reduced scattering coefficient (μ_s')(/mm)		
	530nm	550nm	585nm
Malignant	2.99 ± 0.05	3.62 ± 1.3	3.47 ±1.2
Benign	2.33 ± 0.35	1.99±0.15	1.98±0.56
Normal	2.27 ± 0.35	2.17±0.15	1.97± 0.52

Type of tissue	Value of absorption coefficient (μ_a) (/mm)		
	530nm	550nm	585nm
Malignant	0.16 ± .02	0.12±0.05	0.09 ±0.05
Benign	0.13 ± 0.05	0.11±0.03	0.14±0.05
Normal	0.07 ± 0.02	0.07±0.02	0.05±0.01

Table 3.

as shown in figure 3.17.This is expected because of the high absorption coefficient at that wavelength. Hence it confirms the argument that parallel component retains the intrinsic property of tissue, and the perpendicular component is the one which is more affected by absorption and scattering effects.

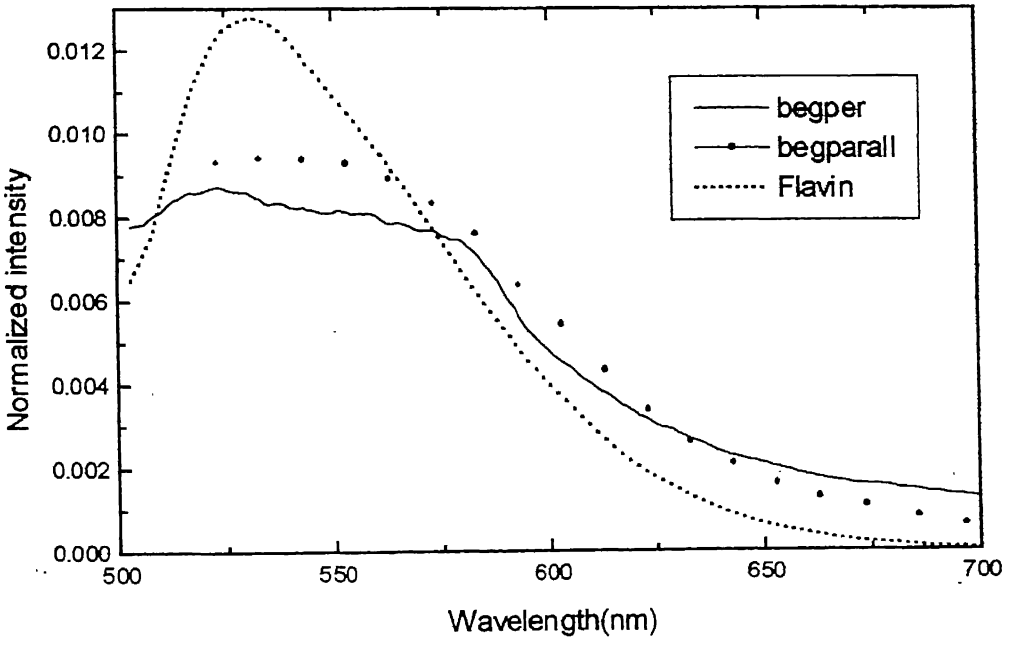

Figure 3.17: average of parallel and perpendicular for all benign cases

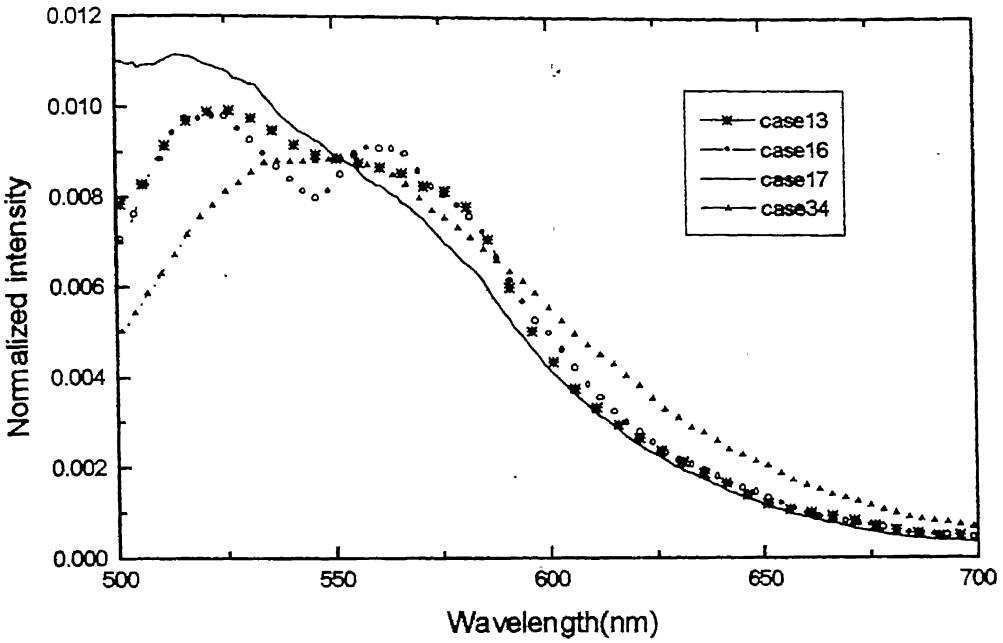

Figure 3.18: Different cases of benign tumors.

The benign breast tumor in most of the cases shows a remarkably prominent peak at ~580nm and profiles appears to be broad with a sharp fall at 590nm in most of the cases. The profiles obtained are a result of 2 major over lapping bands peaked at 515±5 and 565±10nm, with relative intensities and widths of 2 bands are different for different cases. The benign tumor samples were white in color and hence the self-absorption effects by blood may be ruled out. However, whether self-absorption due to any other chromophore affects the profile or not has yet to be studied. To extract more information in this regard, the profiles were fitted to two voigt functions, one peaked at 530nm and the other at 580nm. Assuming the 530 band to be from flavins, the peak positions and FWHM of this band was fitted according to the spectral profiles of the aqueous solution of FAD measured earlier. Based on the explanation given that the parallel component retains the property of the material under study and perpendicular component is more affected by the factors. It is to be noted that all the profiles considered for the calculation of FWHM are the polarized fluorescence spectra (parallel component of fluorescence with polarized excitation).

Quantitatively, from the theoretical fits, a distinct difference was observed in the normal, benign and malignant tumors from the bandwidth of the second voigt band. Figure 3.19 shows the fitted fluorescence spectral profiles for normal, benign and malignant human breast tumors excited at 488nm. To minimise the standard error in the fitting, we have taken 3 voigt functions in normal tissue cases. This third voigt peak is not fixed to nay wavelength, was taken just to fit the background which was an artifact observed in these cases. The bandwidth of normal was seen to be ~33±3nm, out of the 33 normal case studied 4 cases deviated from these values, but within the range of

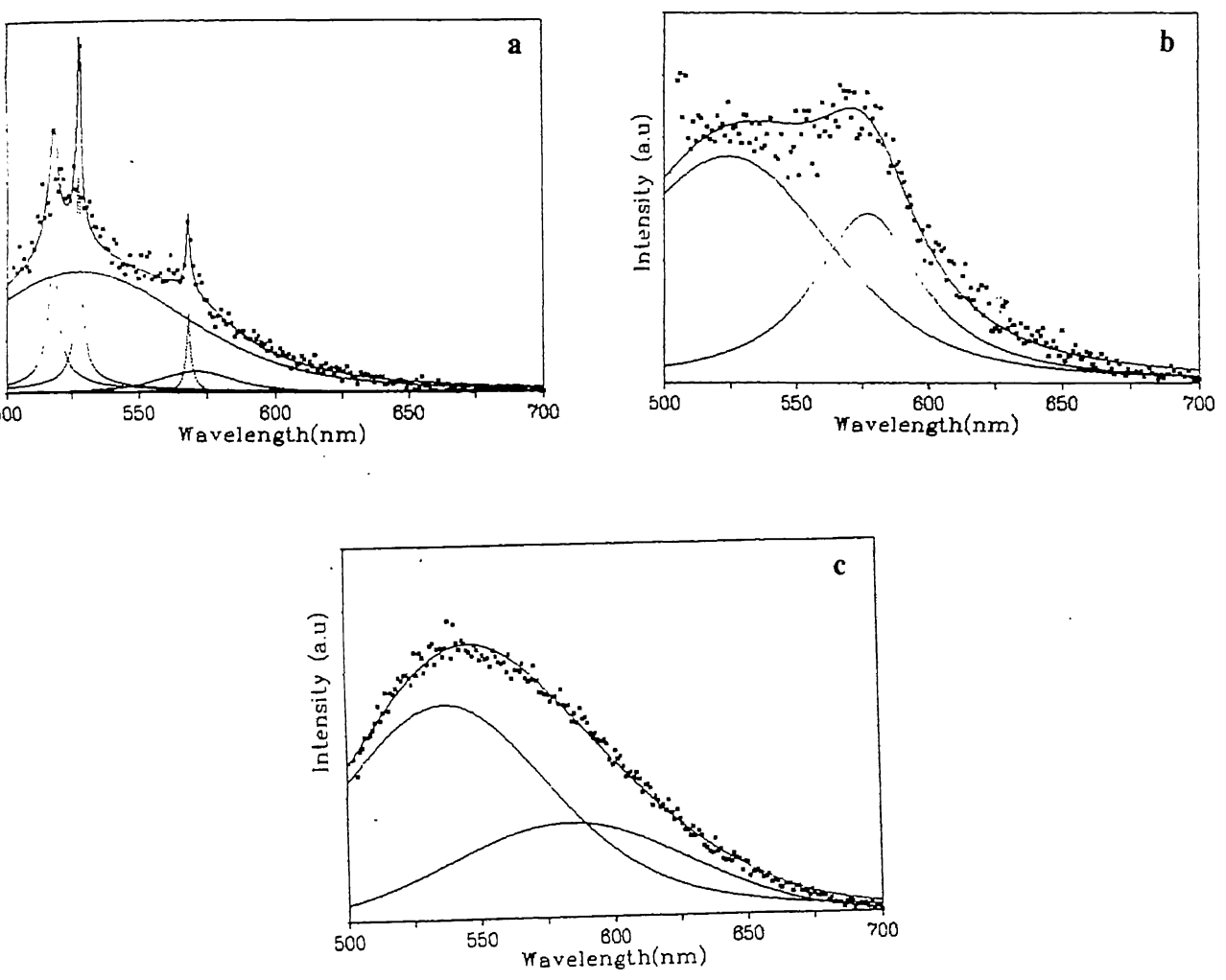

Figure.3.19: Fitted fluorescence spectral profiles for (a) Normal, (b)Benign, (c)Malignant Human Breast tissue.

FWHM as 20-30nm. It was noticed that these cases were more fibrous and white and contained less fat. FWHM of second band for malignant tumors was always greater than 83nm except in case 16, which was a different type of malignant tumor. For benign tumors the FWHM was spread within 30 to 80nm with most of them between were in range 40-65nm. For benign tumors cases which does not contained the sharp fall at 590nm also gave the FWHM in the range mentioned above[11]. Figure 3.18 shows the scatter plot of 35 samples analyzed.

Benign tumors are diseased tissues which are non-cancerous. The different stages of disease may lead to different grades of benign tumors. The benign breast disease includes fibrocystic disease, fibroadenoma, cystosarcoma phylloides and there are other benign disease. In India, the spectrum of benign breast disease also includes specific groups of infection viz. TB, filariasis, etc. It is suspected that the morphological changes inside tissue due to the type of bonding or interaction of the fluorophores or the molecules with various species may be lead to different stage of disease. This may be the reason for not getting a clear cutoff as obtained in normal and malignant tissues.

The broader profiles indicate either presence of another fluorophore or different kinds of flavins[13] in tissue material and their possible interactions with various chemical species present in human breast tissues. Of particular interest is the distinguishing spectral feature of benign tumor, which is pathologically important. The spectral profiles of benign tumors also show an abrupt drop at around 590nm.This could be due to self-absorption effects. The spatial variation of fluorescence intensities have been studied to confirm whether the abrupt decrease is due to self absorption effects in other words, an intrinsic property of tissue. The value of absorption coefficient (as shown in table 3) at 590nm was seen to be higher in benign tumors. Hence the abrupt fall in spectral profile may be due to the self absorption effects caused by different chromophores. The exact nature of these chromophores is yet to be determined.

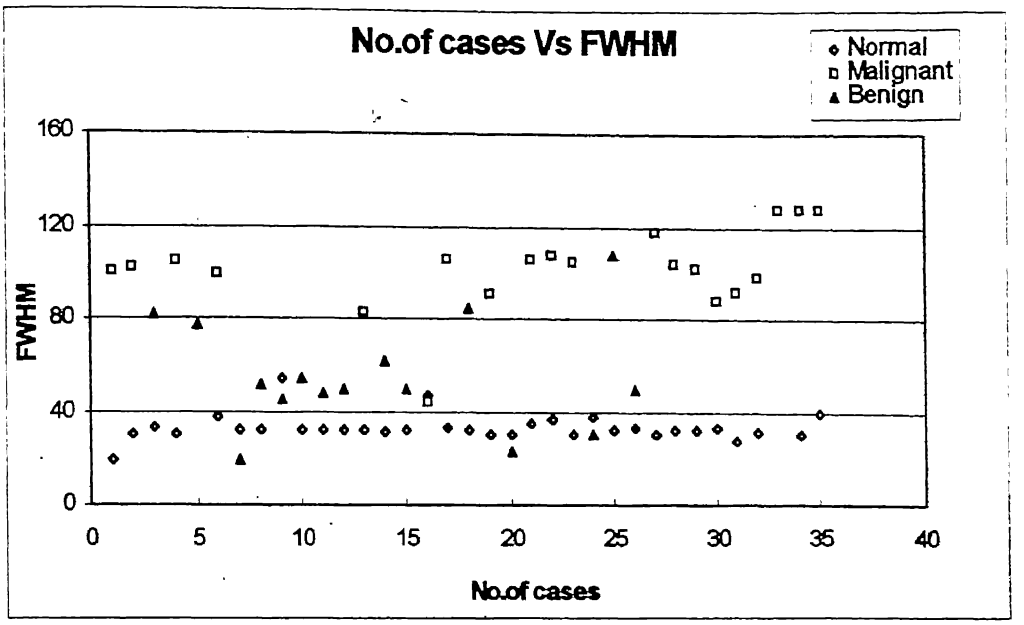

Figure 3.18 Scatter plot of all the cases studied, b) Normal c)Malignant d)Benign human breast tissue.

Table 4 shows the specificity and sensitivity of all the types of tissue based on this analysis. Study shows excellent discrimination among all three types of tissues. Hence polarized fluorescence spectrum can be used as an important diagnostic technique.

Malignant	No. of Samples	20
	Sensitivity	95
	False negative	5
Normal	No. of Samples	33
	Specificity	94
	False Positive	6
Benign	No. of Samples	15
	Sensitivity	86.6
	False negative	33

Table 4.

3.6 *References:*

1. J.R.Lakowicz, "Principles of fluorescence spectroscopy", Plenum Press NewYork, 1983.

2. D.B.Tata, M.Foresti, J.cordero, P.Tomashefsky, R.R.Alfano, M.A.Alfano, "Fluorescence polarization spectroscopy and time resolved fluorescence kinetics of native cancerous and normal rat kidney tissues" , J. Biophys. **50** 463-469, 1986.

3. R.R.Alfano, A.Pradhan and G.C.Tang, "Optical spectroscopic diagnosis of cancer and normal breast tissues", J. Opt. Soc. Am.B , **6** 1015-1023, 1989.

4. R.R.Alfano, G.C.Tang, A.Pradhan, W.Lam, D.C.Choy and E.Ophen, " Fluorescence spectra from cancerous and normal human breast and lung tissues", IEEE J.Quant. Elect.**23** 1806, 1987.

5. T.C.Chia, Z.Huang, W.Zheng, C.Diong, F.S.Choen, " Changes in autofluorescence emission intensities of hunam colonic tissues due to photobleaching process", SPIE **3568** 11-18, 1999.

6. S.G.Demos, A.J.Papadopoulos, H.Savage, A.S.Heerdt, S.Schantz nad R.R.Alfano, " Polarization filter for biomedical tissue optical imaging", Photochem. Photobiol. **66** 821-825, 1997.

7. K.T.Schomancker, J.K.Frisoli, C.C.Compton, T.J.Flotte,J.M.Richter, N.S.Nishioka and T.F.Deutsen, " Ultraviolt laser induced fluorescence of colonic tissue: basic biology and Diagnostic Potential", Laser Surg. Med. **12** 63-78, 1992.

8. C.M.Gardner, S.L.Jacques and A.J.Welch, " Fluorescence spectroscopy of tissue: Recovery of intrinsic fluorescence from measured fluorescence", Applied Optics **35**, 10 1780 1996.

9. J.M. Schmitt, A.H.Gandbakhche and R.F.Bonner, " Use of polarized light to discriminate short-path photons in a multiply scattering medium", Applied Otics **31** 6535-6546 1992.

10.N.Mataga, H.Chosrowjan, Y.Shibata,J.Phys.Chem.B 102 7081, 1998.

11.R.N.Panda, B.V.Laxmi, M.S.Nair, A.Agarwal and A.Pradhan, " Diagnosis of benign breast tumors by fluorescence depolarization and spectral profile analysis", NLS 383, Dec.1999

12. R.R.Alfano, D.B.Tata, J.J.Cardero, P. Tomashefsky, F.W.Lango and M.A.Alfano, "Laser induced fluorescence spectroscopy from native cancerous and normal tissue", IEEE J. Quantum Electron., **20**, pp. 1507, 1984.

13. A.Pradhan, M.S.Nair, N.Ghosh, A.Agarwal, " Spatial variation of fluorescence in human breast tissues", to be printed

CHAPTER 4

4.1 *Introduction*

Biological tissue contains a high density of refractile elements whose size is of the order of the wavelength of light. Therefore individual scattering events are very frequent and eventually scattering is highly anisotropic. Wave mechanics is used in most tissues because of high optical turbidity (like models involving the migration or diffusion of discrete photons) to describe the interaction of light with materials like blood, muscle and bone. Quasielastic light-scattering studies of turbid mediam support the notion that such diffusion or random -walk models can be used to describe the passage of optical radiation through highly multiple-scattering materials [1]. When the mean path length of reemitted photons is short, as is the case for several techniques involving non invasive detection from the surface of illuminating tissues, the random-walk theory may more accurately predict distributions of surface intensity and optical path length than models based on the diffusion equation [2].

Multiple scattering of light from particles in highly scattering media randomizes the direction of propagation and state of polarization. However, polarization memory effect that has been observed in the domain, much larger than the ballaistic region [3] suggests that some information about polarization of the incident light is not lost in the scattering region of propagation. Finally, light propagation in a dense biological tissue becomes depolarized, but one does not know the scale in which this phenomenon occurs. To understand the light propagation through tissues, one should know the nature of tissular components that interact with light at given wavelength and lead to scattering and depolarization. Most of the theoretical studies on multiple light scattering have considered linear, isotropic, homogeneous, non-absorbing media made of non-interacting particles. Mammalian tissues are quite different from such models. However, only a few

papers have been devoted to the forward propagation of light, that can be applied in medicine to investigate thick samples.

The problem of imaging objects such as tumors embedded in healthy breast tissues has motivated the study of polarization, based techniques to discriminate weakly scattered from multiple scattered light [4]. In general, these techniques are based on the assumption that weakly scattered light retains its initial polarization whereas highly scattered light does not. The number of scattering events over which light retains its initial polarization depends on a variety of factors, including the incident polarization state, the size and shape of scatters, the concentration of scatters and refractive indices of the scatters and the surrounding medium.

Teale in 1969 showed the scattering effects on depolarization and in turn also showed that the anisotropy for single scattering is decreased by a factor of 0.7[9]. If in a medium there are "n" number of scattering events faced by the polarized excitation or emission then the resulting anisotropy is reduced by factor $(0.7)^n$ ie. $A_n=A_0*(0.7)^n$, where A_0 is anisotropy without any scattering effects and A_n is anisotropy after n successive scattering events. Based on this theory, in this chapter we have tried to extract more information on the intrinsic anisotropy(Ao) of different breast tissues, by removing the scattering effects. This chapter deals mainly with the 1D and 3D modeling of tissue scattering, by using two different approaches namely diffusion and random walk method.

4.2 *Mathematical Analysis:*

The theoretical model developed to simulate the variation of fluorescence anisotropy with thickness of turbid medium was based on the previous report in which it was shown that each scattering event for both polarized excitation and emission reduces the anisotropy by a factor 0.7. In this section, we analyze mathematically both 1D and 3D models that allows us to demonstrate or arrive at the anisotropy expression in terms of number of scattering events. Part A discribes the 1D approach, and Part B is about 3D approach using lattice model.

Part A:

When the tissue is irradiated with the laser beam, it suffers multiple scattering and absorption along its path inside the medium. The rate of absorption and scattering depend on the excitation wavelength and optical properties of the tissue. These properties in turn depend on several parameters like:

- Scattering mean free path length (l_s).
- The absorption length (l_a).
- The transport mean free path length (l_t).
- The mean cosine of the angle of scattering (g).

The absorption length (l_a) is the mean distance a photon travel in the medium before it is absorbed, so the absorption coefficient $\mu_a = 1/l_a$

The scattering length (l_s) is the mean distance between two scattering events, hence the scattering coefficient is $\mu_s = 1/l_s$.

When light incident on the surface of tissue material , the intensity at any depth z is given by the Bears law:

$$I(z)=I_o \, Exp\{-\mu_{eff} * z)$$

where μ_{eff} is the effective attenuation in the medium.

$$\mu_{eff} = \{3*\mu_a (\mu_a + \mu_s)\}^{0.5}$$

as discussed in the introduction , the anisotropy decreases by 0.7 factor for each scattering. Hence, the anisotropy of fluorescence from a fluorophore located at a distance z from the surface of a medium will be $A_0*(0.7)^{z(\mu s+\mu's)}$. This is because the number of scattering events occuring within the distance z will be μ_s*z for excitation wavelength, and similarly μ'_s*z (for the emission wavelength). where μ_s and μ'_s are the scattering coefficients for excitation and emission wavelength.

Therefore, the total number of scattering which are considered are $(\mu_s+\mu_s)*z$

The anisotropy of fluorescence from fluorophores embedded homogeneously in turbid medium of thickness "t" can now be worked out by giving intensity weightage to fractional contribution of anisotropy from different depths[5].

The fluorescence anisotropy is:

$$A_{obs} = A_o \frac{{}_0\int^t I_o \, Exp\{-\mu^t_{eff} * z\} * (0.7)^n \, dz}{{}_0\int^t I_o \, Exp\{-\mu_{eff} * z\} \, dz} \quad \text{.....(a)}$$

where A_o is the value of anisotropy without any scattering, μ^t_{eff} is the total attenuation coefficient at excitation and emission wavelengths.

Part B:

The model presented here is based on, photon behaviour as a random walker in a lattice. The lattice spacing L is chosen to be the distance between two successive scattering events(mean free path ls). Hence first scattering occurs within the first layer of scattering centers, having applied to the absorption along its path. The absorption coefficient μ in this approach is the absorption per unit step, ie. $\mu = \mu_a * L = \mu_a/\mu_s$, where the scattering is assumed to be isotropic(ie. all scattering direction are equally probable).

Photons are assumed to be inputed at a single point on the surface and collected or about area around that point. The z = 0 layer is an homogeneous absorbing barrier, and the photons emitted from the surface are assumed not to return to the scattering medium.

The probability that a photon will reach r(x,y,z) starting at (0,0,0) in the n^{th} step(n scattering events) is given by [6]:

$$P_n(r) = (3/2\pi n)^{3/2} \, Exp[-3/2\pi \, (x^2 + y^2 + z^2)]$$

$Q_n(r)$ is the probability that the photon is at r(x,y,z) after step n. since z=0 is the perfect absorbing , $Q_n(r)$ is subjected to the boundary condition :

$$Q_n(x,y,0)=0$$

The photons are injected into the medium along the z axis and experience their first collision at the lattice point (x=0, y=0, z=1) have been subjected to absorption while traveling. Therefore,

$$Q_n(r) = e^{-\mu n} \{ P_{n-1}(x, y, z-1) - P_{n+1}(x, y, z+1)\}$$

$$Q_n(r) = e^{-\mu n} \{ P_{n-1}(x, y, z-1) - P_{n+1}(x, y, z+1)\}$$

The probability that a photon will be absorbed at step n at the point $\rho = (x, y)$ on the surface is given by :

$$\Gamma(n, \rho) = 1/6\, Q_{n-1}(x, y, 1)\, e^{-\mu n}$$

Hence the expected number of steps taken by the photon before it is reemitted at the surface $z = 0$, is defined by:

$$\langle n \rangle = \Sigma\, n\, \Gamma(n, \rho) / \Sigma\, \Gamma(n, \rho)$$

which upon substitution leads to the following expression

$$\langle n \rangle = 2 + \rho \sqrt{(3/2\mu)}\, \{ a / b\},$$

where, $a = \{1 - \mathrm{Exp}[\sqrt{(6\mu)}\, \{ \rho - \sqrt{(\rho^2 + 4)}\}]\}$

$b = \{1 - \rho / \sqrt{(\rho^2 + 4)} * \mathrm{Exp}[\sqrt{(6\mu)}\, \{ \rho - \sqrt{(\rho^2 + 4)}\}]\}$

which is given by the equation 16 in ref. [6].

This is integrated over ρ from 0 to 1, which is the collection surface area, in the experiments carried out by us.

We have considered that the fluorescence photon is the one, which is propagating in the scattering medium. The same analysis is used here, except for the wavelength (λ) chosen.

The fluorescent light which travels less path than the scattering light and hence the A_o (intrinsic anisotropy) obtained from this analysis would be higher then it should be. To account for this, we have taken :

$$A_{obs} = A_o * k * (0.7)^{\langle n \rangle} \qquad \ldots\ldots\ldots\ldots\ldots\ldots (b)$$

where the k factor (dimensionless) , is expected to be greater then 1 to take care the intensity variation. In other words, without this k factor (>1), our 3D Model would have calculated <n> more than what it is, as fluorescent light is created beneath the incident plane rather on the surface plane, so it travels less path compared to the light

created at the incident plane (surface of the sample). The validity of the model developed was checked in tissue phantoms.

4.3 *Experimental Method:*

The experimental setup is shown in Figure 2.1 in chapter 2. Experiments were carried out on tissue phantoms prepared with different known concentrations of FAD (Flavin Adenine Dinucleotide) as fluorophores and polystyrene microspheres as scatterers. The concentration of FAD was of the order ~ μM. The absorption coefficient for these solutions were measured with the help of spectrophotometer. Scattering coefficients of the tissue phantoms corresponding to different microspheres were calculated using Mie's theory, as follows:-

$\mu_s = N \pi a^2 Q'_s$, where N is the concentration of the scatteres ,

a is the radius of the scatter (here polystyrene microspheres),

Q'_s is the scattering extinction coefficient.

Initially, fluorescence was recorded from only for FAD solution (30 μM) (as explained in chapter 2) to obtain the intrinsic anisotropy Ao. Next concentration of FAD was fixed and by varying the concentration of microspheres in the range of 10^{10} to 10^9/cc different solutions were obtained. The polarized fluorescence of these phantoms were recorded.

Another set of measurements was taken by adding an absorber as methylene blue to increase the absorption coefficient of the solutions. For this solution with methylene blue the Ao value was found by repeating the experiment with out scatteres, ie, only FAD and methylene blue of 50μM and 120μM.

4.4 *Results and discussion :*

Ao {intrinsic anisotropy } for 30μM FAD solution was calculated by $(I_{II} - I_{\perp})/(I_{II} + 2I_{\perp})$, where I_{II} and $I_{\perp}$ are parallel and perpendicular components of polarized

fluorescence spectra and found to be 0.102 ±0.005 . It is to be noted that Ao is for the solution which doesn't contain any scatterers, hence depolarization effects due to scatterers are suppressed. Using this value of Ao, table 4.1 shows the anisotropy A_o calculated for different scattering concentrations with 1D model. The value of Ao calculated theoretically is large compared to the Ao observed experimentally, this may be due to experimental errors. And table 4.2 gives the value of Ao for solution A with both 3D and 1D approach. For these calculations eq.(a) and eq.(b) were used. With one dimensional approach the experimental and theoretically calculated values for A_{obs} are in good agreement, but with the 3D approach, it was observed that in 3D A_{obs} follows the exact variation with wavelength as found in 1D calculations. In all the cases this (A_{obs}) value differed by a factor of 2.3 (our k factor) {approx} which was estimated by matching 3D plots with those of 1D plots (for several cases) keeping standard deviation of the differences at minimum.

For solutions 4 and 5 (table 4.1), Ao is found to be very high compared to the experimental value (A_{obs}). This is due to the fact that these solutions contain very large number of scatterer concentration and therefore there are large losses in the collection of fluorescenct light and hence leads to low value A_{obs} .

Sol.	**Scatt.Conc ($\times 10^9$/cc)**	**A_{obs}**	**μ_s (488nm)**	**μ_s (530nm)**	**μ_a (488nm)**	**μ_a (530nm)**	**A_0 theoretical**
sol 1	9.0	0.047	0.4933	0.464	0.0096	0.00054	0.116
sol 2	5.98	0.063	0.3277	0.308	"	"	0.119
sol 3	2.7	0.055	0.148	0.139	"	"	0.108
sol 4	23.6	0.05	1.29	1.22	"	"	0.153
sol 5	50	0.03	2.74	2.58	"	"	0.121
Sol 6	5.28	0.05	0.289	0.273	"	"	0.114

Table 4.1 Intrinsic anisotropy for different scattering concentration at FAD concentration 30μM theoretical (1D) and experimental values.

solution A:

λ-nm	μ_s (/mm)	μ_a (/mm)	A_{obs}	A_0 (1D)	A_0 (3D)	A_0(FAD+MB) (experimental)
488	0.178	0.0512				
530	0.167	0.0549	0.05	0.065	0.144	0.065
540	0.167	0.0715	0.064	0.082	0.178	0.0561
550	0.1669	0.0586	0.033	0.053	0.0943	0.056
560	0.1663	0.077	0.0423	0.054	0.116	0.032
570	0.1653	0.1045	0.03	0.0375	0.0797	0.038
585	0.1634	0.276	0.025	0.029	0.06	0.03

Table 4.2 Intrinsic anisotropy for solution A(scatterers 3.25×10^9/cc and FAD at 50μM and methylene blue at 120μM) claculated using 1D and 3D approach.

As λ increases, Ao is observed to decrease for the solution A (which contains methylene blue) as shown in Figure 4.1. Similar decrease was observed in all other solutions. The abrupt discrepancies in the analysis of 540nm and 560nm of solution A cannot be explained. So ignoring these points, our theoretical data matched with the experimental ones as shown below. Figure 4.1(a) is with all the points, and (b) is after removing points at 540 and 560nm, which matches excellently.

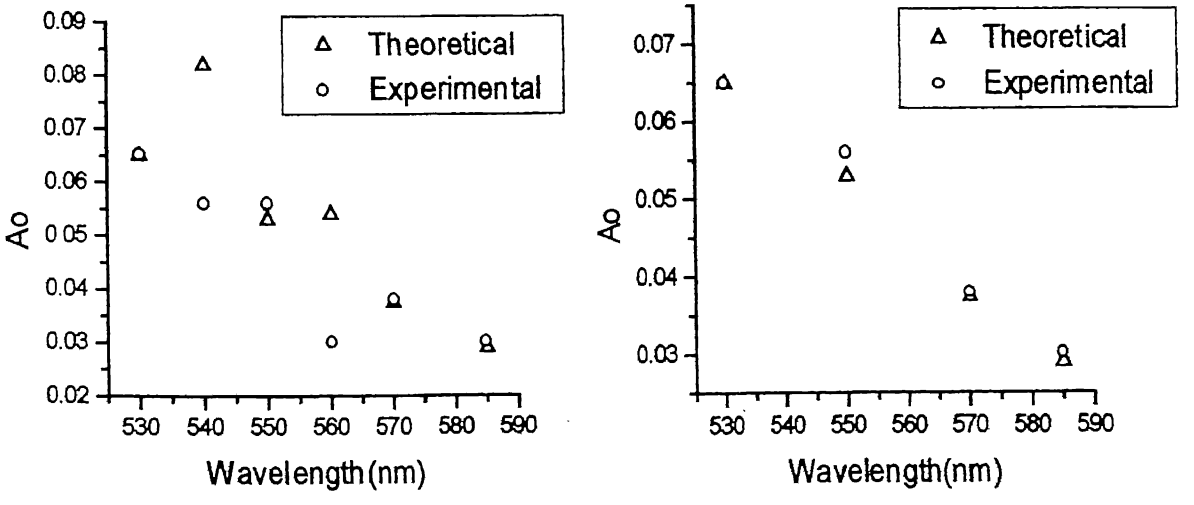

Figure 4.1 Ao vs. wavelength for solution A.

Hence this model can be used for calculating the intrinsic anisotropy of both tumor and normal tissues. With this idea, we obtained Ao values at different wavelengths for all the 6 cases of human breast tissue, both with 1D and 3D Model, which were in good agreement after incorporating the k factor 2.3 in our 3D Model. As shown in the Fig 4.2 for a typical case.).

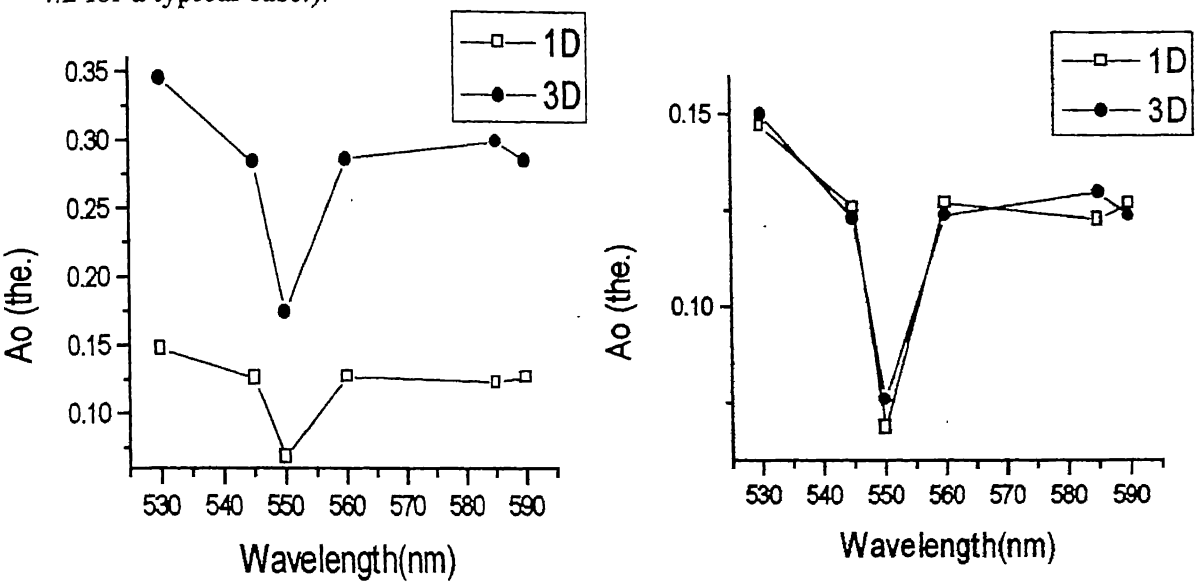

Figure 4.2 a) plot of 3D and 1D without normalizing, b) with normalizing by factor 2.3

It was found in all the cases that Ao for normal tissues was always higher than tumor at 530 nm which is in good agreement with the previous report[7]. This may be because in tumor tissues the density of cells is large therefore there is less depolarization due to rotational motions, but the energy transfer to other fluorophores is more probable leading to low anisotropy values. Except for the case no. 13, which was an benign and the FWHM for this case was coming to be below FWHM of normal leading to conclude that this case is an abnormal one. Case no.1 is an exception but this case also displayed discrepancy in spectral profile.

Table 4.2 shows Ao values (1D as well 3D) for all cases at 530. It's difficult to make any conclusion on the variation of Ao with wavelength as in tissues there are large no. of molecules which affect the environment of the tissue medium (like absorber, haemoglobin etc). The concentration of the absorber is the main factor in depolarization

of the fluorophores apart from scattering depolarization [8], which varies from tissue to tissue. The binding of flavins with other molecules and pH variation also affects Ao.

Case no.	Ao for Tumor Tissue		Ao for Normal Tissue	
	1D	3D	1D	3D
1	0.371	0.403	0.179	0.183
2	0.069	0.074	0.147	0.15
3	0.198	0.2	0.233	0.21
4	0.105	0.116	0.213	0.191
5	0.139	0.146	0.153	0.15
6	0.144	0.148	0.137	0.139

Table4.3: Intrinsic anisotropy calculated using 1D and 3D approach for normal and tumor breast tissues at 530nm.

Hence, this may be the reason for not getting a clear cutoff for intrinsic anisotropy Ao. This work is preliminary and further studies with large no. of cases studied there is a possibility of getting a cutoff value of Ao of atleast for tumor tissues. Figure 4.3 shows variation Ao values for all the tumor cases studied with wavelength.

This analysis was extended to the thickness variation in 4 cases of human breast tissues with thickness varying from 4mm to 0.5mm. Table 4.3 shows the Ao calculated for thickness of 4mm, 1mm and 0.5mm, both in 3D and 1D. In going from thick to thin, it

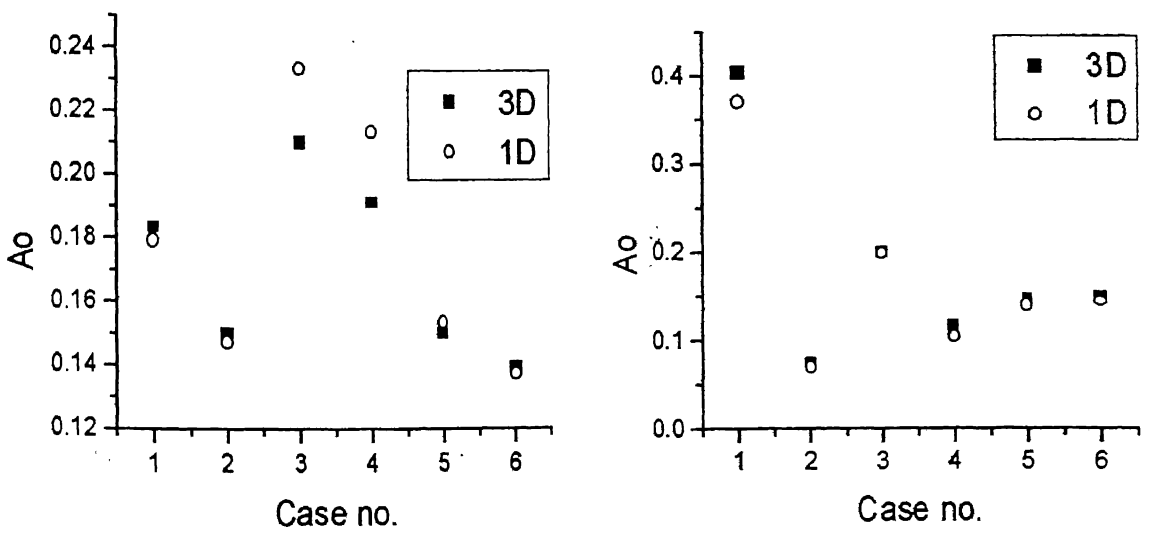

Figure 4.2: Ao vs. case no. a) for all the normal breast tissues , b) for all the tumor breast tissues.

was found that for 3 cases there was a cross over of the Ao for normal tissues. With the change in thickness from 4mm to 0.5mm we are actually reducing the scattering effects, and hence we expect that the value of Ao (does not depend on scattering properties) to be constant for both the tissues. This is not reflected in our results. The reason being that, anisotropy is very sensitive to the environment and the number of fluorophores that are

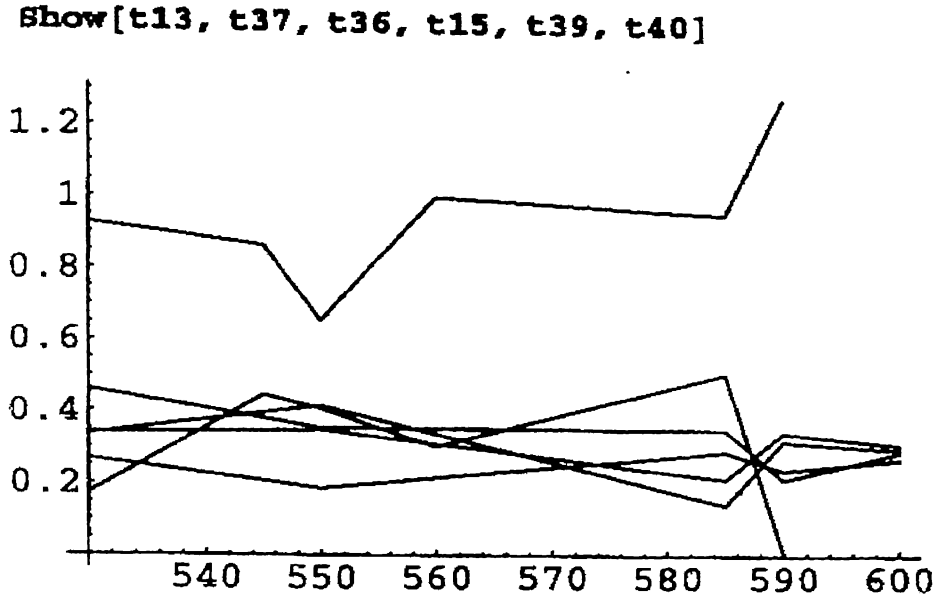

Figure 4.3 variation of Ao values for all the tumor cases studied with wavelength.

contributing to the fluorescence emission. The ratio of number of fluorophores to number of scatters, appears to play a major role at thicknesses comparable to the mean free path length.

To obtain information on this aspect, experiments were performed by varying the FAD concentration, keeping the scattering concentration constant. It was found that the anisotropy decreases with increasing the concentration of fluorophores [8]. This experiment shows change in anisotropy with the ratio defined above, hence this factor is very important when we are dealing with thin tissues. All the cases considered here are showing deviation from the results we discussed in chapter3 for the variation of

tissues. All the cases considered here are showing deviation from the results we discussed in chapter3 for the variation of anisotropy with thickness. More cases have to studied to explain this artifact of decrease in anisotropy of tumors from 1mm to 0.5mm. This may also be the reason for not getting a clear cutoff value of Ao(intrinsic).

Tumor cases

case no.	Thickness	μ_a	μ_s	$A_{observed}$	$A_0^{theoretical}(3D)$	$A_0^{theoretical}(1D)$
43	-	-	-	-	-	
	1mm	0.063	1.77	0.117	0.204	0.194
	0.5mm	`	`	0.078	0.137	0.13
37	4mm	0.084	1.846	0.1	0.168	0.164
	1mm	`	`	0.1	0.168	0.164
	0.5mm	`	`	0.064	0.107	0.105
38	4mm	0.05	4.64	0.13	0.26	0.24
	1mm	`	`	0.07	0.14	0.13
	0.5mm	`	`	0.09	0.18	0.166
39	4mm	0.056	1.847	0.069	0.12	0.115
	1mm	`	`	0.06	0.106	0.1
	0.5mm	`	`	0.08	0.142	0.133

.....

Normal cases

case no.	Thickness	μ_a	μ_s	$A_{observed}$	$A_0^{theoretical}(3D)$	$A_0^{theoretical}(1D)$
43	-	-	-	-	-	
	1mm	0.109	3.17	0.13	0.23	0.22
	0.5mm	`	`	0.138	0.24	0.235
37	4mm	0.123	7.16	0.07	0.135	0.134
	1mm	`	`	0.1	0.19	0.19
	0.5mm	`	`	0.19	0.365	0.364
38	4mm	0.05	7.24	0.138	0.29	0.28
	1mm	`	`	0.113	0.24	0.23
	0.5mm	`	`	0.113	0.24	0.23
39	4mm	0.149	9.84	0.084	0.164	0.17
	1mm	`	`	0.144	0.28	0.29
	0.5mm	`	`	0.083	0.162	0.167

Table 4.3

There are three major reasons for depolarization (rotational motions, the energy transfer and multiple scattering), when one of the factor is removed (multiple scattering)

the intrinsic anisotropy of the normal is observed to higher than the tumor tissues. This observation shows that the depolarization due to other factors is large in tumor tissues than normal. With large number of cases studied a cutoff can be obtained.

To conclude both 1D and 3D models have worked reasonably, and this model can be used as a new technique for diagnosis in human breast tissues and can be extended to other types of tissues.

4.5 *References:*

1. D.J.Pine, D.A.Weitz, J.X.Zhu and E.Herbolzheimer,"Diffusing - Wave spectroscopy: dynamic light scattering in the multiple scattering limit", J.Phys.(paris) **51**,2101 , 1990.

2. A.H.Gandjbakhche, R.Nossal nad R.F.Bonner, " Scaling relation ships for theories of anisotropic random walks applied to tissue optics", App. Opt. **32** No. 4, 504,1993.

3. D.Bicout, C.Brosseau, A.S.Martinez and J.M.Schmitt, "Depolarization of multiple scattered waves by spherical diffusers : influence of size parameter", Phys. Rev. E **49**, 1767, 1994.

4. J.M.Schmitt, a.H.Gandbakhche and R.F.Bonner," Use of polarized light to discriminate short-path photons in a multiply scattering medium", Appl. Opt. **31**, 6535, 1992.

5. S.k.Mohanty, N.Ghosh, S.K.Majumder and P.K.Gupta, "Fluorescence depolarization by light scattering in human breast tissues", NLS proceedings, 381, 1999.

6. R.F.Bonner, R.Nosal, S.Havlin and G.H.Weiss, " Model for photon migration in turbid bilogical media ", J. Opt. Soc. Am.A, **4**, 423, 1987.

7. D.B.Tata, M.Foresti, J.cordero, P.Tomashefsky, R.R.Alfano, M.A.Alfano, "Fluorescence polarization spectroscopy and time resolved fluorescence kinetics of native cancerous and normal rat kidney tissues" , J. Biophys. **50** 463-469, 1986.

8. J.R.Lakowicz, "Principles of fluorescence spectroscopy", 1983

9. L.W.Teale, " Fluorescence depolarizatin by light- scattering in turbid solutions", Photoche. Photobiol. **10**, 463, 1969.

CHAPTER 5

5.1 *Conclusion:*

In this project, fluorescence spectroscopy studies were applied to human breast tissues. In-vitro studies with visible excitation, the characteristic information from the shape of profiles and depolarization effects are considered.

The environmental effects on flavin molecule have been studied with visible excitation. Spectroscopic differences between the cancerous and normal tissues have been experimentally demonstrated. Fatty normal tissues displayed three Raman peaks and profile showed a dip at 550nm. In the malignant tissue cases the fluorescence profile displayed a monotonous decrease in intensity without any dip. In benign tissues the profiles were broad which is the result of two major overlapping bands peaked at around 530±10nm and 565±10nm, and in most of the cases there was a abrupt fall of intensity at 590nm. This abrupt fall in spectral profiles may be due to high the self absorption effects caused by different chomophores.

Polarized fluorescence spectral profiles and anisotropy studies on malignant, benign and normal human breast tissues show a definite distinction between these tissues. The distinction is mainly based on FWHM of the second band at 580nm. Normal tissues displayed a narrow bandwidth of 33±3nm, compared to malignant tissues which showed the bandwidth to be greater than 85nm. In benign tissues this value lies in the range of 40-84nm. The large variation may be due to varying contributions of another fluorophore or another species of flavin in different cases and yet to confirmed.

The qualitative information on the local environment surrounding the fluorophores within normal and cancerous tissues was reflected in the fluorescence depolarization studies were the anisotropy (depolarization factor) for tumors is observed to be higher than the normal counterparts. Absorption effects are more dominant at thick

tissue chunks, where the scattering effects are saturated for both the types of breast tissues.

Thin sections show distinct difference in scattering effects between normal and tumor tissues, leading to expected higher anisotropy of normal tissues. The thickness variation studies show that the multiple scattering effects dominates in thin tissue section, higher anisotropy of tumors in thick tissue suggests there is less difference in scattering effects between normal and tumor, but other effects play a major role.

With the theoretical modeling in 1D and 3D the intrinsic anisotropy of the human tissues can be obtained. Higher intrinsic anisotropy of normal tissue suggests that depolarization due to rotational motion and the energy transfer is more dominant here. This technique can be used as a polarization imaging, with the normal tissue showing higher anisotropy.

To conclude, the characteristic information from shape of the fluorescence spectra and depolarization effects can provide a very good discrimination between cancerous, normal and malignant breast tissues in the visible region. The results therefore suggest that a polarized fluorescence spectral profiles can itself provide excellent discrimination between malignant and benign which is of pathological importance. This preliminary study also draws attention to the effects of multiple scattering and fluorescence concentration in fluorescence depolarization of tissues. this work shows the begniing of a more organised study with tissue phantoms and simulations to further understand the molecular aspects in disease development by polarization fluorescence.

5.2 *Scope for Future work.*

1. Further analysis can done on the polarized fluorescence spectral profiles to get the intrinsic profiles of the biomedical material under study. The difference in parallel and perpendicular can give more information on the environment of tissues.
2. The anisotropy with thickness variation can be studied in detail to obtain the exact crossover of anisotropy of normal and tumor.

3. The trend of anisotropy variation at very thin tissues (microlevel) should be studied to know the effect of concentration of fluorophores to that of scatterers in the depolarization.
4. In theoretical modeling the assumption that only fluorescence photon is getting affected by scattering is to be modified.
5. This research work can be extended to detect the cancer of different organs to see if this kind of excellent discrimination occurs there too.